12–13). Aliquots of the organic layer were periodically removed, passed through a short column of neutral alumina, and analyzed for oxidation products by gas chromatography using a 5% phenyl methyl silicone capillary column (10 m × 0.53 mm) with PhBr as an internal standard.

Determination of the Optical Purity of *trans*-β-Methylstyrene Oxide. A sample of *trans*-β-methylstyrene oxide (2–3 mg) obtained from the oxidation above with dissolved in $CDCl_3$ (0.3 mL), and solid portions of shift reagent tris[3-[(heptafluoropropyl)hydroxymethylene]-*d*-camphorato]europium(III) were added incrementally until a desired separation of the methyl, α-, and/or β-proton signals in the ^1H NMR spectrum of the epoxide was obtained. Integration of the fully separated enantiomeric peaks was used to determine the enantiomeric purity of the epoxide. Each experiment showed essentially equal intensities of all enantiomeric pairs of protons.

Acknowledgment. Support of this work by grants from the National Institutes of Health (GM-34841) and the National Science Foundation (CHE-8706616) is gratefully acknowledged. We also thank Dr. C. K. Cheung and Prof. W. J. le Noble for assistance with high-pressure experiments and Prof. E. Kimura for a gift of compound **2d**.

Registry No. **2a**, 119274-66-7; **2b**, 119296-11-6; **2c**, 119274-67-8; **3a**, 119296-12-7; **3b**, 119274-68-9; **3c**, 119274-69-0; **3d**, 78737-53-8; **4a**, 94405-01-3; **4a**·4HCl, 119274-70-3; **4b**, 119274-71-4; **4b**·4HCl, 119274-72-5; **4c**, 94405-03-5; **4c**·4HCl, 119274-73-6; **5a**, 3397-32-8; **5b**, 3397-35-1; **5c**, 3496-11-5; **6a**, 83852-28-2; **6b**, 119274-74-7; **6c**, 119274-75-8; **7a**, 83852-29-3; **7b**, 119274-76-9; **7c**, 110465-49-1; PhCHO, 100-52-7; 1,3-diaminopropane, 109-76-2; dimethyl malonate, 108-59-8; *trans*-β-methylstyrene, 873-66-5; *trans*-β-methylstyrene oxide, 23355-97-7.

Rational Design of Templates for Intramolecular O,N-Acyl Transfer via Medium-Sized Cyclic Intermediates Derived from L-Cysteine. Definition of an Experimental Maximum in Effective Molarity through the Study of "Tunable" Templates

D. S. Kemp,* Robert I. Carey, John C. Dewan, Nicholas G. Galakatos, Daniel Kerkman, and See-Lap Leung

Department of Chemistry, Room 18-584, Massachusetts Institute of Technology, Cambridge, Massachusetts 02139

Received September 17, 1987

Rate constants and effective molarities for intramolecular O,N-acyl transfer have been measured for a series of unsymmetrical disulfides derived from cysteine and having the general structure H-Cys(S-XY-OAc)-OMe, for which XY is a rigid molecular spacing element that maintains a fixed OS distance lying in the range of 4.5–6.5 Å. A synthetic route is described to 4-hydroxy-6-mercaptodibenzothiophene, involving lithiation of 4-methoxydibenzothiophene followed by reaction with elemental sulfur and positional isomer separation. A maximum effective molarity (EM) value of 5 M is seen for the 4,6-disubstituted dibenzofuran function (OS = 5.45 Å) while EM values of less than 0.1 M are seen for 4,6-disubstituted phenoxathiin and 4,6-disubstituted dibenzothiophene functions (OS = 3.90 and 6.30 Å, respectively). Distance calculations and estimates of strain energy based on torsional and van der Waals terms are used to show that this result is consistent with a cyclic transition state containing one conformation of the cysteine framework. Energy minimization calculations were carried out by using a novel null-vector procedure for finding allowed torsional motions. They imply that the transition state for O,N-acyl transfer is strained by ca. 6 kcal/mol in the dibenzofuran case.

In earlier reports[1,2] we have described progress toward a new methodology for the chemical ligation of medium-sized polypeptides. A central issue throughout this work has been the rational design of a spacing element or template that can permit intramolecular O,N-acyl transfer across the cysteine disulfide function of **1**. After synthesis and study of 10 distinct molecular frameworks, we have attained effective molarity (EM) values of 5–10 M for templates derived from 4,6-difunctionalized dibenzofurans.

Developing a new type of practical acylation chemistry has led us to consider a variety of fundamental problems connected with entropy-induced rate acceleration.[4,5] In this paper we present a detailed analysis of our results to date on the optimization of size and shape of spacers that facilitate the reaction **1** → **2** → **3** as well as new results that define an experimental maximum in EM as a function of spacer length. A simple energy minimization analysis is used to interpret these results and to predict a maximum EM value that might be obtained by using an optimal template belonging to this structural series.

Underlying Issues. Effective molarity can be estimated when an intramolecular reaction involving a reactive pair of atoms can be successfully modeled by an intermolecular reaction in which the pair of reactive groups appear in separate molecules. Formally, EM is the ratio of first- and second-order rate constants for these reactions and is equal to the concentration of the external nucleophile that must be added to the intramolecular reaction mixture to permit inter- and intramolecular processes to proceed at equal rates. More than 15 years ago in a paper concerned with the role of entropy in enzymatic catalysis, Page and Jencks[4] related the EM values that can be observed for intramolecular reactions that generate small,

(1) Kemp, D.; Galakatos, N. *J. Org. Chem.* **1986**, *51*, 1821–1829. Kemp, D.; Galakatos, N.; Dranginis, S.; Ashton, C.; Fotouhi, N.; Curran, T. *Ibid.* **1986**, *51*, 3320.
(2) Kemp, D. *Biopolymers* **1981**, *20*, 1793.
(3) Kemp, D.; Kerkman, D.; Leung, S.-L.; Hanson, G. *J. Org. Chem.* **1981**, *46*, 490. Kemp, D.; Galakatos, N.; Bowen, B.; Tan, K. *J. Org. Chem.* **1986**, *51*, 1829–1838.
(4) Page, M.; Jencks, W. *Proc. Natl. Acad. Sci. U.S.A.* **1971**, *68*, 1678.
(5) Kirby, A. *Adv. Phys. Org. Chem.* **1980**, *17*, 183.

0022-3263/89/1954-1589$01.50/0

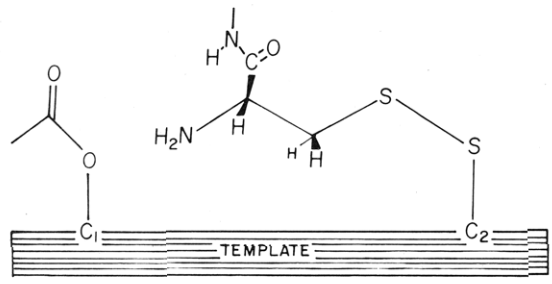

1

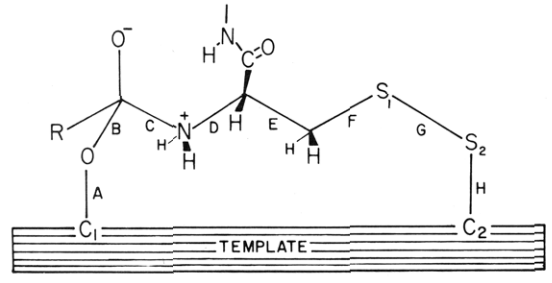

2

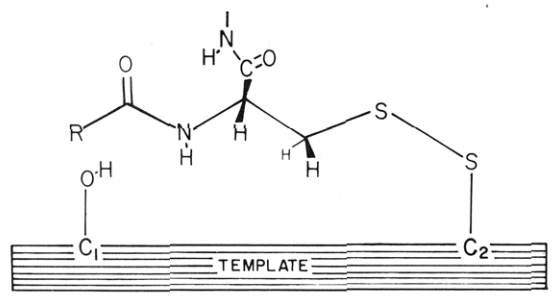

3

relatively unstrained rings to the theoretical rate accelerations expected for reactions in the gas phase in which translational and rotational degrees of freedom have been frozen. They concluded that EM values of roughly 10^8 M are to be expected for rigidly constrained intramolecular reactions, and as noted in the recent review by Kirby,[6] experimental values up to or exceeding this value have been frequently observed.

When the choice of an appropriate intramolecular model reaction is difficult, ambiguities attend the interpretation of EM values. Kirby[6] has stressed that an EM value of 10^{10} M or more may be taken as evidence for strain which is unique to the starting material for the intramolecular reaction, which is relieved in the cyclic product, and which is not present in the model reaction. For small systems that show very large EM values, solvation or conformational features that are unique to the intramolecular reaction may make the choice of a suitable intermolecular model essentially impossible. Page[5] has reviewed many of the structural factors that can distort EM values and reduce their interpretability; he also cites arguments that solvation differences between the transition states of model and substrate should not distort EM values. In view of the large rate effects that can result in protic solvents from even small changes in solvation of nucleophilic lone pairs[7] and the likelihood that solvent bound between paired reacting groups behaves differently from bulk solvent, we find these arguments unpersuasive. Although not free of

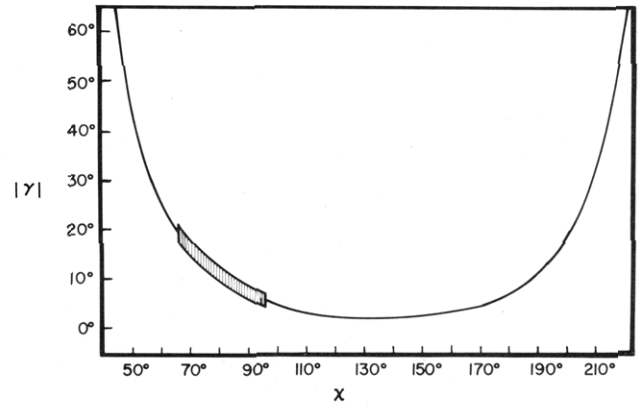

Figure 1. The change in the absolute value of the dihedral angle $OC_1C_2S_2 = \gamma$ with change in the disulfide torsional angle = χ for conformation **23**. The shaded part of the graph is the region of minimum energy for the disulfide bond.

these problems, the examples of disulfide bond formation provided by Creighton and Goldenberg[8] for oxidation of thiol functions in the small protein BPTI may well provide the best estimate of the range of EM values to be expected between a pair of reactive groups in an entropically constrained environment. For bond formation between the sulfur atoms of Cys 5 and Cys 55, which appear in the highly constrained protein core, an EM value of 5×10^5 M is seen, while S–S bond formation involving Cys 14 and Cys 38, which lie near the surface of the protein, yields an EM value of only 2×10^2 M. We have used these values as rough guidelines in pursuing the studies described below.

Doubts concerning the relationship between intramolecular and model reactions are minimal if both transition states can assume the same conformations and if the nucleophilic and electrophilic atoms of both starting materials can be surrounded by independent solvation spheres. In planning further studies of EM values we were therefore led to consider cyclization reactions in which nucleophile and electrophile lie at the ends of a relatively long chain of atoms. Thus, correlation of EM value with structure for a series of templates that bridge atoms C_1 and C_2 of **1** seemed to us to offer the following rewarding features. First, because the distance between the span of atoms is relatively long, it should be straightforward to find a mechanistically relevant intermolecular model reaction. Second, with isolated exception, EM values for substrates containing chains of six or more freely rotating bonds are quite small, and neither theory nor experiment provides a reliable prediction for the upper bound on EM values that can be realized in solution for such reacting systems. Test cases that may approximate bounds of this type seemed to us particularly interesting because practical applications can result from successful optimization experiments involving relatively large molecular frameworks.[1,2] Third, large distances can be more easily modeled by tunable spacing elements in which small variations in template geometry can be used to vary spacer length, and tunable systems of this type should be particularly suited for modeling using energy minimization algorithms.

Designing templates that span long bonded linkages raises a series of difficult questions involving the effects of bond length and rigidity on EM. An intriguing thought experiment involving bond length is to imagine that all bonds of a molecule such as **4** could be doubled in length with no change in molecular force constants. What would

(6) Page, M. *Chem. Soc. Rev.* **1973**, *2*, 295–323.
(7) Parker, A. *Chem. Rev.* **1969**, *69*, 1. Olmstead, W.; Brauman, J. *J. Am. Chem. Soc.* **1977**, *99*, 4219. Nodelman, N.; Martin, J. *Ibid.* **1976**, *98*, 6597.
(8) Goldenberg, D.; Creighton, T. *J. Mol. Biol.* **1984**, *179*, 527–545.

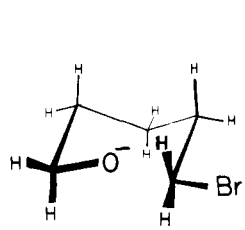

4, EM = 280 M

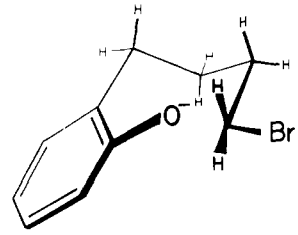

5 = EM = 118 M

be the resulting change in EM? This question can be answered for reactions in the gas phase, but there seems to be no obvious theoretical or intuitive answer for reactions in a discrete, structured solvent. A more practical question concerns the likely change in EM when only one bond such as the C–O⁻ of **4** is replaced by a rigid multiply bonded linkage such as the *o*-C_6H_4–O⁻ function of **5**. As Dunitz has noted for carbocyclic systems, replacement of a methylene by a 1,2(*Z*)-alkene function often generates cognate pairs of structures.[9] Such a change leaves constant the number of freely rotating bonds that link the electrophile and nucleophile but alters the size of the formed ring and the geometry of the reactive atoms. Since several key parameters have been simultaneously varied, it is difficult to draw conclusions from a single example of such a substitution. However, typified by **4** and **5** (each of which contains four freely rotating bonds), the handful of such pairs that can be found in the data cited by Kirby[6] show small (2–10-fold) EM variations that can be either positive or negative and that appear to be randomly distributed. Tentatively, therefore, substitution of a rigid, larger spacer for a bond leaves the EM value nearly unchanged, as expected from the entropy arguments of Page and Jencks.[4] The rigid group effect has been recently review by Mandolini.[10]

These results are drawn from reactions that generate relatively small rings. One can ask if the high conformational degeneracy of a multiatom linkage such as that of **2** might not be more successfully accommodate by a flexible spacer. A simplified, two-dimensional form of the challenge that a flexible transition state poses for a molecular architect is seen in Figure 1, which graphs for a particular conformation of **2** the variations of the dihedral angle defined by the terminal bonds A and H with changes in the disulfide torsional angle. A flexible spacer that is constrained to be planar could only accommodate conformations of **2** that have dihedral angles near 0. A flexible spacer that allows independent variation of dihedral angle and OS_2 distance would sample all points of the graph without any bias toward the region of minimum energy, which must lie in the shaded part of the plot. Unconstrained flexibility thus fails on two counts; first, it samples large regions of conformational space that the transition state cannot enter, and second, it fails to weight those parts of conformational space that are accessible energetically and are therefore significant entropically. A flexible spacer would be advantageous only if it could function cooperatively, by sampling only the regions of minimum energy while also mirrowing changes in the transition state of both angles and distances.

The design of cooperatively flexible templates is an intriguing concept that may provide the only strategy that can yield very large EM values for reactions generating medium-sized rings. Because of the geometrical constraints of small molecules, this strategy is probably impractical for the organic chemist; however, it may eventually lie within the scope of enzyme bioengineering.

Results: EM Values for Template-Bridged Reactions 1 → 3. Dependence of EM on Template Structure. The aim of these studies is construction of templates that can be attached to the terminal atoms of **1** to optimize conversion to **3**. As described in detail in the next section, we have used tetrahedral intermediate **2** as a model for the structure of the rate-determining transition state for the reaction. Templates were identified that appear to be capable of bridging the termini of **2**, the corresponding compounds **1** were synthesized, and evidence was sought for a concentration-independent O,N-acyl transfer reaction to form **3**, for which a first-order rate constant k_1 could be measured. A corresponding monofunctionalized template was synthesized, for which the second-order rate constant k_2 for the reaction **6** → **7** was measured, and an

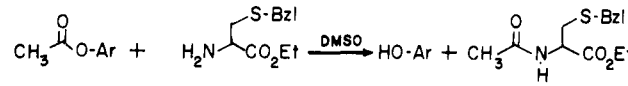

6 **7**

EM value was calculated as k_1/k_2. For practical reasons arising from the requirements of the thiol capture strategy, the esters **6** must all be phenolic esters of a very weakly activated class, corresponding to esters of phenols that are lacking in electron-withdrawing substituents. Typical half-times for the conversion of **6** to **7** in the rate-accelerating solvent DMSO lie in the range of 10–30 h at amine concentrations in the 0.1–0.5 M range. Under these conditions in DMSO, the reactions are typically first order in amine concentration.

Since very slow intramolecular reactions of **1** to **3** are complicated by disulfide interchange, half-times of greater than 200 h are difficult to establish unambiguously, and correspondingly, EM values of below 0.1 M are experimentally indistinguishable from 0. We are interested in three categories of EM values for intramolecular reactions: values at or below 0.1, for which no intramolecular reaction can be convincingly shown; values in the range of 0.1–0.3, which correspond to inefficient intramolecular reactivity; and values above 1 M, which correspond to reactivity that is both interesting and potentially useful. In this section we report our experimental findings, which provide a coarse-grained but model-independent picture of the structural requirements for intramolecular versions of the reaction **1** → **3**. (Discussions of rate analyses and the selection of intermolecular models appear in the Experimental Section.)

Two template distances O–S and C_1–C_2 of **3** are particularly useful in analyzing the experimental findings. The most compact conformations of **2** are characterized by O–S distances as short as 2.7 Å, while in the most extended conformation the O–S distance is 7.9 Å. Clearly a very diverse class of templates must be examined if a fair sampling of the possible conformations of **2** is to be carried out. The templates that we have prepared and studied to date are reported in Table I, together with calculated bridging distances O–S_2 and C_1–C_2 as defined in **1**. In Figure 2, pairs of these distances are plotted to identify the portion of this two-dimensional conformational space that is sampled by each of these structures. Rigid structures appear as points, while structures that permit variations in either or both distances appear as boxes for which the area is an approximate indicator of the degree of flexibility of the template. Solid or shaded points or boxes are used to symbolize species **1** that undergo observable intramolecular O,N-acyl transfer, while species

(9) Dunitz, J.; Waser, J. *J. Am. Chem. Soc.* **1972**, *94*, 5645.
(10) Mandolini, L. *Adv. Phys. Org. Chem.* **1986**, *22*, 46–49.

Table I.[a] Templates for the Reaction 1 → 3

symbol	template	mercaptophenol corresp to 1	C_1–C_2, Å	O–S_2, Å
A	**9**	2-mercaptophenol[b]	1.40	2.98
B		1-hydroxy-8-mercaptonaphthalene[c]	2.45	2.42
C	**8**	2-(mercaptoethyl)phenol[b]	2.53	2.5–4.2
D		*o*-hydroxy-*o'*-mercaptobiphenyl[d]	3.1–3.8	2.9–5.2
E	**10**	4-hydroxy-8-(mercaptoethyl)xanthene[b]	4.16	2.6–5.4
F	**13**	4-hydroxy-6-mercaptophenoxathiin[e]	4.35	3.90
G	**11**	4-hydroxy-5,7-dimethoxy-6-methyl-8-mercaptoxanthone[b]	4.76	4.81
H	**12**	4-hydroxy-6-mercaptodibenzofuran[e]	4.82	5.45
I	**14**	4-hydroxy-6-mercaptodibenzothiophene[b]	5.23	6.30
J		*p*-hydroxy-*p''*-(mercaptomethy)-*o*-terphenyl[d]	6.6–6.7	5.6–9.0

[a] See Figure 2. [b] Synthesis and kinetics are reported in this paper. [c] Synthesis and kinetics are reported in ref 11. [d] Synthesis and kinetics are reported in ref 12. [e] Synthesis and kinetics are reported in ref 3.

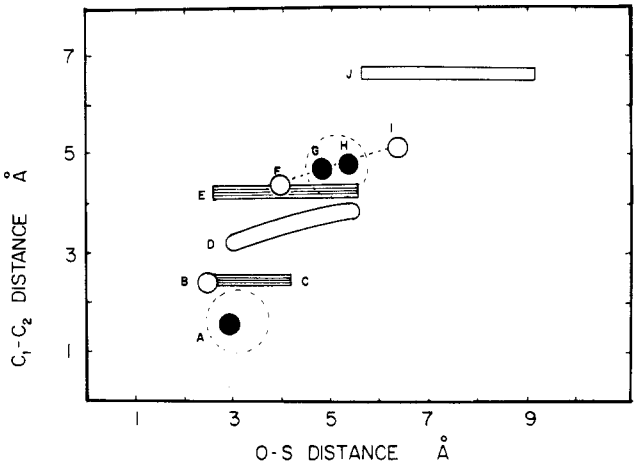

Figure 2. A ranking of the templates of Table I with respect to their capacity for sustaining intramolecular catalysis. Black circles correspond to efficient templates; shaded boxes, to inefficient templates.

for which no intramolecular transfer could be detected appear as open circles or boxes.

As seen from Figure 2, with an important qualification flexible templates fail to give detectable intramolecular reactivity. The two exceptions are the (mercaptomethyl)arene derivatives C = **8** and E = **10**, which strikingly exhibit relatively large EM values. These are the most structurally constrained of the five flexible templates since for each the C–C bond distance is fixed. Another

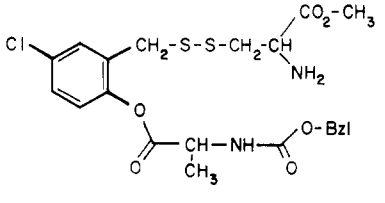

8

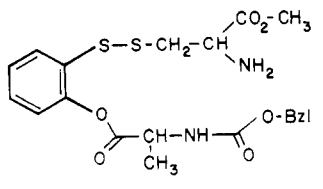

9

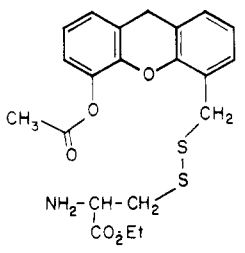

10

feature may be more important. Each of these structures lies close to a region of the graph assigned to a rigid template that permits a facile intramolecular reaction. Strikingly, there appear to be two such regions, symbolized by the dotted circles in Figure 2. The first lies in the vicinity of point A and corresponds to **9**, and the second lies near points G and H and corresponds to **11** and **12**. Since a line connecting these regions nearly touches coordinates of several templates for which no intramolecular reactivity could be detected, it is very likely that the two regions must be associated with two distinct conformations of the transition state for the acyl transfer reaction.

A fine-grained study of templates for this reaction should thus partition the C_1–C_2, O–S_2 plane into a small number of noncontiguous patches, each defined by an observable intramolecular reaction and each imbedded in a continuum of paired distance parameters corresponding to templates for which intramolecular reactivity is not observed. Each patch should correspond to an accessible conformation (or a set of structurally related conformations) of the transition state for the reaction, and its relative area should give a measure of the flexibility of the conformation. In Menger's usage, each patch may correspond to a particular reaction window among possible transition states for the reaction.[13] A first step in constructing such a graph is to construct templates with distance parameters that neighbor the points that correspond to significant intramolecular reactivity.

The point at 3.0, 1.4 corresponds to the *o*-phenylene template A = **9**. Unfortunately, this region of the graph is defined by short distances for which the choice of templates is very limited. The data points in the vicinity of 5.0, 4.8 are in a structurally more versatile region, and we have prepared and studied the series of structurally cognate templates **11**, **12**, **13**, and **14** to define the length of this acyl transfer permissive patch.

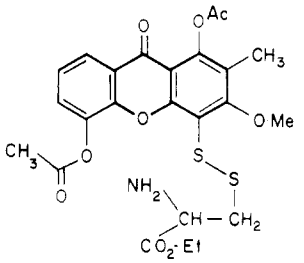

11

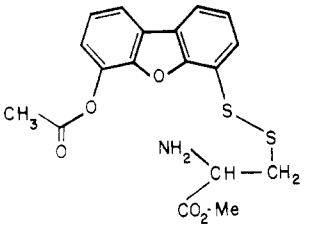

12

Strikingly, as seen from the data in Table II and Figure 2, **11** and **12** show significant EM values, but **13** and **14** react in DMSO solution at 0.001 M concentration largely by intermolecular mechanisms, as evidenced by a second-order dependence of the observed rate constant on

(11) Kemp, D.; Leung, S.-L.; Kerkman, D. *Tetrahedron Lett.* **1981**, *22*, 181.
(12) Hanson, G.; Kemp, D. *J. Org. Chem.* **1981**, *46*, 5441.
(13) Menger, F. *Tetrahedron* **1983**, *39*, 1013.

Table II. EM Values for Templates That Exhibit Intramolecular Reactivity

structure	EM value,[a] M
A = 9	0.08–1.3[b,c]
C = 8	0.5–10[b,c]
E = 10	3–14[c]
F = 13	<0.1[d]
G = 11	0.5–0.7
H = 12	4–10[e]

[a] DMSO, 25 °C. [b] Proximity of the ortho substituents makes choice of a substrate for the intermolecular reaction problematic. [c] Range is attributable to uncertainties in the rate constant; disulfide interchange complicated this slow reaction. [d] Both inter- and intramolecular reactivity is observed. [e] EM values are those found for a range of 1-substituted derivatives.[3]

Table III. Distance and Angle Data from X-ray Crystal Structure Analysis of 4-Methoxy-6-mercaptodibenzofuran (15)[a]

bond distances, Å (esd)		bond angles, deg (esd)	
SC_1	1.770 (3)		
C_1C_{12}	1.384 (5)	SC_1C_{12}	121.9 (2)
$C_{12}O_1$	1.379 (4)	$C_1C_{12}O_1$	124.1 (3)
O_1C_{11}	1.380 (4)	$C_{12}O_1C_{11}$	104.9 (2)
$C_{11}C_{10}$	1.393 (5)	$O_1C_{11}C_{10}$	124.4 (3)
$C_{10}O_2$	1.366 (5)	$C_{11}C_{10}O_2$	116.4 (3)

[a] The complete listing of bond and angle data appears in the supplementary material.

substrate concentration. The EM values for these species must be considerably less than 0.1 M.

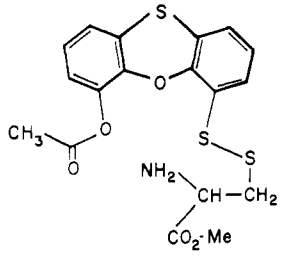

13

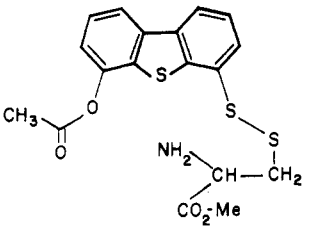

14

X-ray structures for the unsubstituted heterocycles corresponding to each of these four templates 11–14 have been reported.[14-17] Unfortunately, these do not provide the critical bond angles that define the attachment of the oxygen and sulfur atoms to the heterocyclic nucleus. In the above structures, the corresponding angles involving hydrogen substituents can deviate significantly from the expected value of 120°, and as a result, we carried out an X-ray structural study of **15**, which corresponds to the template for which efficient intramolecular acyl transfer was observed. The results of this study are given in Table III.

As is apparent from the data of Table III, in **15** the OCC but not the SCC angle indeed deviates from 120° and the ether oxygen bends toward the neighboring heterocyclic oxygen by −3.6°, a key point since the O–S template spacing distance is very sensitive to the values for these angles. We have used the Cambridge Data Base to identify other examples of part structure **16**. A mean deviation

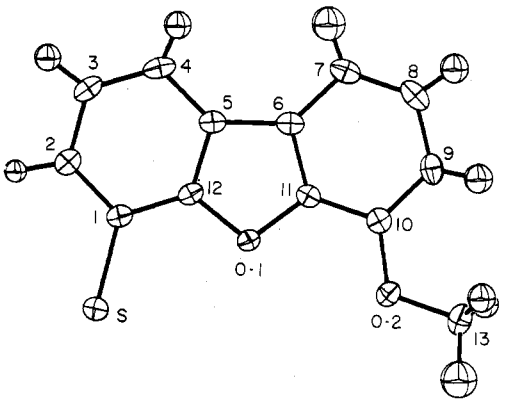

15

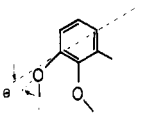

16

from 120°, $\theta = -1.9°$ with a range of +2 to −6° was observed for the five available examples.

We assume that the values seen for dibenzofuran hold for the xanthone, phenoxathiin, and dibenzothiophene structures as well, and under this assumption, comparisons of the relative size and shape of the four templates are provided by **17**, **18**, and **19**, in which the exact atomic positions of the phenoxathiin, xanthone, and dibenzothiophene frameworks are, respectively, superimposed on those for dibenzofuran. In the case of the nonplanar phenoxathiin, a projection onto the dibenzofuran plane is shown.

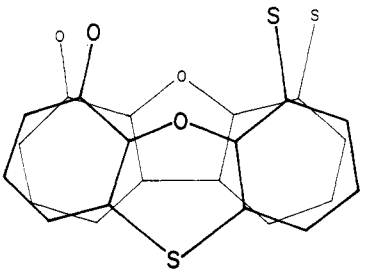

17

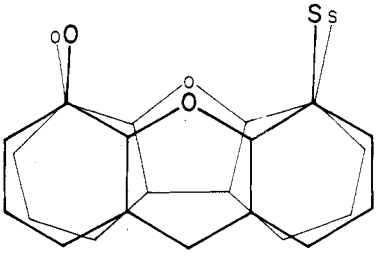

18

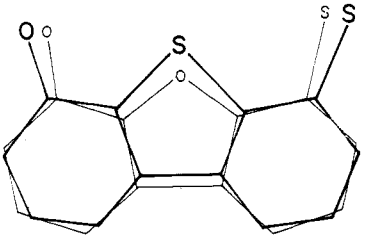

19

(14) Burland, D. *J. Chem. Phys.* **1981**, *75*, 2635–2642. Stout, G.; Shun Lin, T.; Singh, I. *Tetrahedron* **1969**, *25*, 1975–1983.
(15) Banerjee, A. *Acta Crystallogr., Sect. B* **1973**, *B29*, 2070.
(16) Hosoya, S. *Acta Crystallogr.* **1966**, *20*, 429–432.
(17) Schaffrin, R.; Trotter, J. *J. Chem. Soc. A* **1970**, 1561–1565.

From these observations and results, it is clear that for the 4.8, 5.0 Å acyl transfer "window", the value of EM is very sensitive to the length of the spacing element. Intramolecular acyl transfer is seen only for the xanthone (G) and dibenzofuran (H) cases, and the substrates E = **13** and I = **14** react largely by an intermolecular pathway, even at high dilution.

This picture is of course oversimplified. The "fit" of a given template to the transition state for the reaction is characterized not just by C_1–C_2 and O–S distances but by six structural parameters of which four are independent: the two distance parameters, together with two bond angles, one dihedral angle, and a van der Waals interaction term that describes the contact between cysteine and template atoms. Appearance of the two distance parameters of a template within an allowed area of the graph is therefore a necessary but not a sufficient condition for observable intramolecular reactivity, and a more detailed analysis is required to establish sufficiency. In the next sections we consider the basic issues that arise in such an analysis. The most important questions that can be addressed are whether the EM value observed for **12** can be significantly increased, and if so, what changes in geometry are likely to result in such an increase.

Molecular Modeling for Conformations of the Transition State for the Acyl Transfer Reaction 1 → 3. The results of the preceding section provide a coarse, template-based picture of two regions of the C_1–C_2, O–S_2 plane for which intramolecular acyl transfer can occur. In this section we revisit the C_1–C_2, O–S_2 plane by examining the possible conformations of the cysteine backbone of the transition state for the acyl transfer reaction. By comparison of the experimental results of the preceding section with the models to be developed here, it should be possible to define the geometry of the template-bridged transition state and probe its destabilizing structural features, with the aim of increasing acyl transfer efficiency through further modifications in template structure.

The available evidence implies that the transition state for the reaction **1** → **3** closely resembles **2**. Although isolated examples exist of acyl transfer reactions that proceed by mechanisms other than the familiar addition–elimination process that forms a tetrahedral intermediate,[18] these appear to require good leaving groups and are therefore very unlikely to provide the path of lowest energy for an O,N-acyl transfer reaction involving an oxyanion-destabilizing dipolar aprotic solvent (DMSO) and a relatively poor leaving group. As noted by Jencks et al.[19] and by Menger,[20] the rate-determining transition state for acyl transfer reactions of this kind appears to contain a fully formed C–N bond, nearly tetrahedral geometries at the acyl carbon and amine nitrogen, and partially broken N–H and C–OPh bonds. The breaking N–H bond is almost certainly strongly hydrogen bonded to a single molecule of DMSO.[21] Kemp, Choong, and Peakar have noted that the pattern of steric effects seen for 25 reactions in which the size of substituents at both the ester and the amine sites is systematically varied is only consistent with substantial steric bulk and presumed tetrahedral character at both acyl carbon and amine nitrogen.[22] Estimates of the energy differences between the intermediate and the rate-determining transition state for reactions of this type lie in the range of 8–15 kcal/mol,[23] which corresponds to only a 0.1–0.3-Å change in a bond length in the hypothetical case that all the observed energy change results from the stretching of the bond to the leaving group. Our approach to modeling the structure of conformations of the transition state for **1** → **3** is to construct a framework for the intermediate **2** by using known structural parameters for the cysteine disulfide moiety and assuming normal lengths and angles for the region of reacting bonds, as shown in **20**, which may be compared with structure **2**. As with **2**, the linked bonds of **20** are identified with letters A–H, starting with the C_1–O bond on the left of the structure.

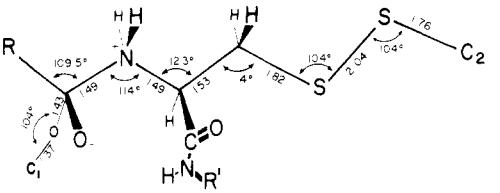

20

Construction of a rank ordering of the stable conformations of **20** requires knowledge of torsional angle energetics, which, with the important exception of the torsional angle at the leaving group, can be assigned at least approximately by analogy with simpler systems. Structural data from both X-ray and neutron diffraction experiments are available for one crystal form of LL-cystine,[24] and X-ray data alone are available for five simple cysteine derivatives.[25] These have been used for the corresponding distance and bond angle coordinates for **20**, along with standard values for the C–O and C–N bond lengths in the reacting bond region. Bond angles in the reacting bond region are assigned standard tetrahedral values for their type of hydrogen substitution.

To a first approximation, the torsional potential energy functions at bonds B–G determine the relative stabilities of the conformtions of **20**. As noted by Allinger,[26] torsional barriers at bonds connecting tetrahedral atoms substituted solely with carbon and hydrogen atoms are substantially higher than for substitutions involving oxygen or bivalent sulfur. Of the three bonds of **2** = **20** that link tetrahedrally substituted atoms, C and D are thus likely to have the highest torsional barriers. As seen in **21a** and **21b**, the two preferred conformations at bond D differ primarily in gauche interactions of the bulky acyl carbon with acyl or methylenethio functions. A 1,2-gauche interaction between an acyl carbon and a methyl group is ca. 0.4 kcal/mol less destabilizing than the corresponding interaction between two methyl groups. (Gauche *n*-butane is 0.9 kcal/mol less stable than trans, but the corresponding difference for butyric acid is 0.5 kcal/mol.[27]) Data for an analogous comparison for a group bulkier than methyl are not available, but the energy difference between **21a** and **21b** is likely to be substantially greater.

Allinger notes that, in methyl ethyl disulfide, trans and gauche orientations at the CH_2–S bond are nearly equally stable,[28] which suggests that the three staggered rotamers at bonds E and F may be also of comparable stability. Strikingly, in the crystal structures of cystine, torsional

(18) Ugi, I.; Beck, F.; Fetzer, U. *Chem. Ber.* **1962**, *95*, 126.
(19) Fersht, A.; Jencks, W. *J. Am. Chem. Soc.* **1972**, *94*, 4733.
(20) Menger, F.; Smith, J. *J. Am. Chem. Soc.* **1972**, *94*, 3824.
(21) Su, C.; Watson, J. *J. Am. Chem. Soc.* **1974**, *96*, 1854.
(22) Kemp, D.; Choong, S.; Pekaar, J. *J. Org. Chem.* **1974**, *39*, 3841.
(23) Guthrie, J. *Acc. Chem. Res.* **1983**, *16*, 122. Guthrie, J. *J. Am. Chem. Soc.* **1978**, *100*, 5892.
(24) Jones, D.; Bernal, I.; Frey, M.; Koetzle, T. *Acta Crystallogr., Sect. B* **1974**, *30*, 1220.
(25) Pattabha, V.; Srinivasan, R. *Int. J. Pept. Protein Res.* **1976**, *8*, 27.
(26) Allinger, N. *Adv. Phys. Org. Chem.* **1976**, *13*, 17. Allinger, N.; Kao, J.; Chang, H.-M.; Boyd, D. *Tetrahedron* **1976**, *32*, 2867.
(27) Allinger, N.; Chang, H.-M. *Tetrahedron* **1977**, *33*, 156.
(28) Allinger, N.; Hickey, M.; Kao, J. *J. Am. Chem. Soc.* **1976**, *98*, 2741.

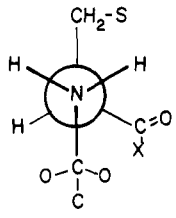

21a

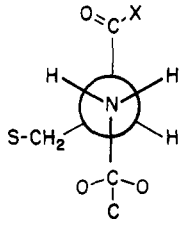

21b

angles of +69.4° and +89.2° respectively are observed[24] for the equivalent bonds. For the cystine structures, and S–S dihedral angle (bond G of **2**) has an average absolute value of +78.1 ± 5.0°; 13 values for the dihedral angles of disulfides found in five proteins show a significantly higher mean: +85.6 ± 26.1°. The large standard deviation for the latter reflects the total range of values from +31° to +113°. Although the disulfide dihedral angle has substantial energetic constraint, it appears to be remarkably tolerant of moderate distortions from the textbook value of 90°, a point that has been noted by Allinger, who calls attention to uncertainties in the potential barrier at this bond.[28]

Barriers at bonds B and C pose special problems, since these are respectively the breaking and forming bonds of the reaction, and this region of the transition state is likely to be highly solvated. We assume that the torsional barrier at the breaking bond B is negligible, and from our earlier studies of the steric effects for O,N-acyl transfer reactions, we conclude that the trans rotamer at bond C is energetically preferred.[22]

Considering only preferred staggered orientations at bonds C–G, one sees that 36 = 1 × 2 × 3 × 3 × 2 relatively stable conformations are possible in principle for **20**, and treating orientation at the breaking bond B as a free parameter, one finds that, for 11 of these, bonds A and G can be so oriented that bridging by a template is possible without severe steric interaction with other atoms of the cysteine backbone. These eleven bridgeable cases are defined by the torsional angles at bonds C–G that are listed in Table IV.

The five potentially bridgeable conformations of **19** that are of lowest energy are depicted in structures **22–26**. The intrinsic geometries and the variations of torsional angle energetics result in substantially different degrees of flexibility. For example, the most compact conformation, **26**, has the most variable OS_2 distance, largely because changes in the torsional angles have an unusually large effect on the terminal distance parameters. Conformations **23** and **24** differ only in the sign of the terminal dihedral angles B and G. A significant difference is their orientation at the breaking bond, which for **24** corresponds approximately to the s-cis configuration of the starting ester. The four conformations **22**, **23**, **25**, and **26** correspond to an s-trans configuration at that bond.

A two-dimensional graph is a useful way to visualize these conformations. In Figure 3, the five accessible regions of C_1–C_2, O–S_2 distances are plotted, and in Figure 4, this graph is superimposed on the data of Figure 2 that correspond to templates for which intramolecular reactivity is observed. From this superimposition it is evident that conformation **23** is unique in corresponding to the C_1–C_2, O–S_2 distances of the xanthone and dibenzofuran templates **11** and **12** for which reasonably efficient intramolecular catalysis can be observed. The reactive template patch in the vicinity of 3.0, 1.4 Å corresponds to the *o*-phenylene template **9** and must be assigned to a distorted form of the conformation **26**, as seen in the cyclic structure **27**.

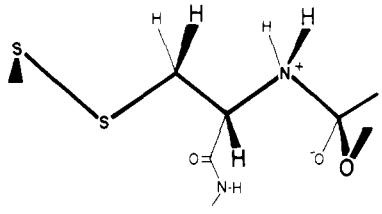

22

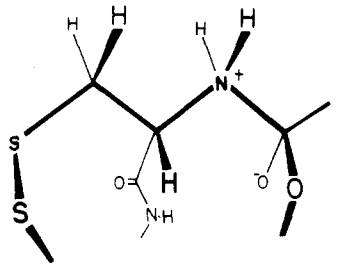

23

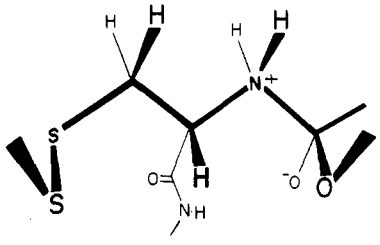

24

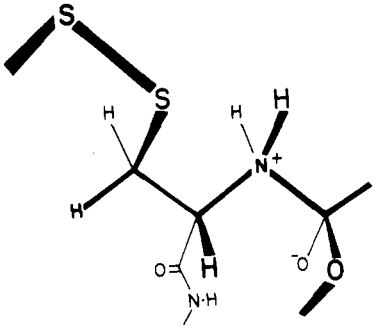

25

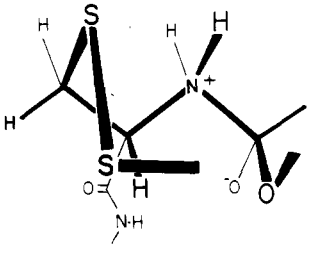

26

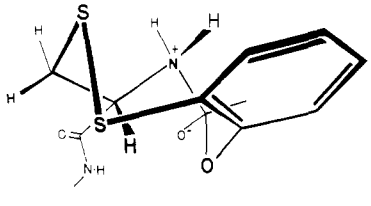

27

For rigid templates, the dibenzofuran **12** exhibits the largest EM value we have thus far observed, and it is therefore of particular interest to evaluate the torsional and van der Waals strain for the fitting of the 4,6-disub-

Table IV. Bridgeable Conformations of 20 = 2

no.	dihedral angles at bonds C–G of **2**	O–S_2 distance, Å
1 = **22**	−60, 180, 180, 180, −90	7.22
2 = **23**	−60, 180, 180, +60, −90	5.24
3 = **24**	−60, 180, 180, +60, +90	5.24
4 = **25**	−60, 180, −60, 180, +90	6.82
5 = **26**	−60, 180, −60, −60, +90	4.56
6	−60, +60, 180, 180, −90	4.85
7	−60, +60, +60, 180, +90	4.16
8	−60, +60, +60, −60, −90	2.57
9	−60, +60, +60, +60, +90	4.95
10	−60, −60, 180, −60, −90	4.86, 4.64
11	−60, −60, +60, +60, −90	3.37, 2.88

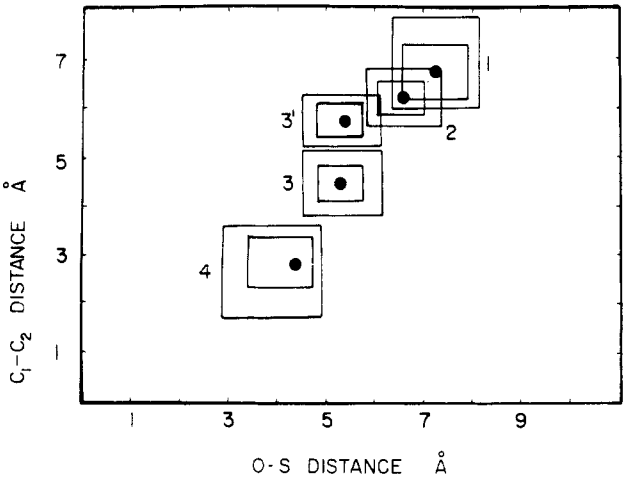

Figure 3. A comparison of the distances between terminal atoms of the conformations **22–26**. Black dots correspond to the precise distance parameters of the conformation. The inner box corresponds approximately to an energy minimum; the outer box identifies less accessible space.

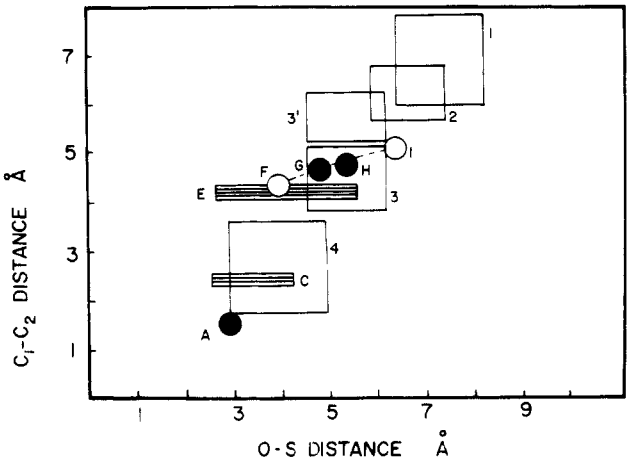

Figure 4. A superimposition of Figures 2 and 3. The efficient templates G and H must allow reaction via conformation **23**, and template A must allow reaction via a distorted form of conformation **26**.

stituted dibenzofurano function to its unique matching conformation **23**. As may be seen in the two views of **28a** and **28b**, the C_1–C_2 and O–S_2 distances of the dibenzofuran template can be exactly accommodated by a set of torsional angles that are close to those of conformation **23**: B, 117.2°; C, 61.5°; D, 182.3°; E, 188.2°; F, 60.7°; G, 98.0°. Structure **28ab** represents a molecule with 55 kcal/mol of van der Waals strain, largely resulting from the contact between the α-hydrogen of the cysteine framework and the heterocyclic oxygen. Using the torsional angle values given in Table IV, one can calculate an α-H···O distance of 1.54 Å and an α-C···O distance of 2.29 Å, both of which are substantially within the van der Waals repulsive regions for the respective atoms. Significantly, for any torsional motions of the cyclic structure **28**, the distances between any of the heterocyclic atoms and the cysteine α-C, β-C, and N and their respective H atoms are always at least 0.8 Å shorter than those involving any of the other cysteine atoms; these atoms therefore largely define the van der Waals strain for the class of cyclic structures resulting from internal torsional motions of **28**.

We have used the following model to carry out a simple

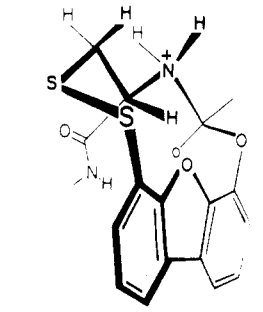

28a

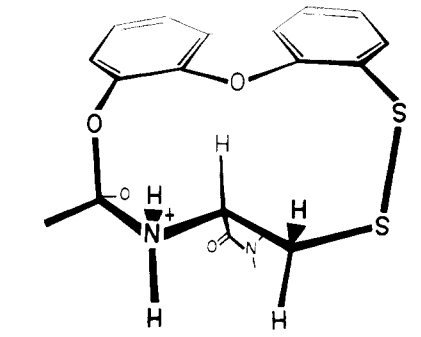

28b

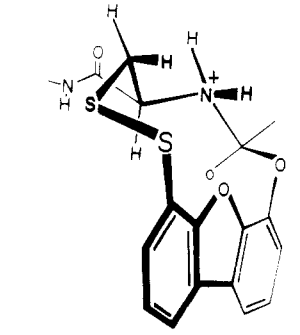

29a

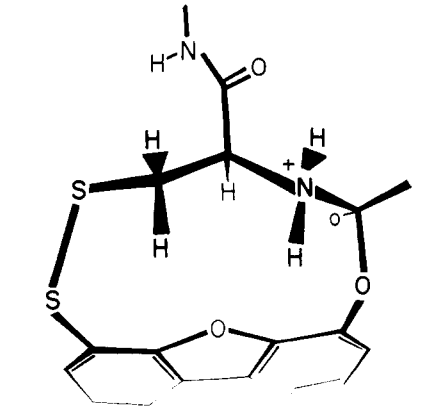

29b

Table V. Calculated Strain Energies for Cyclic Structures 2. Comparisons of Templates 11–14

structure	torsional angle values: B, C, D, E, F, G	C_1–C_2, Å; $\angle OC_1C_2$, deg	O–S_2, Å; $\angle C_1C_2S_2$, deg	strain energy
13	139.5, 83.4, 152.0, 129.0, 58.5, 121.7 (phenoxathiin)	4.41; 80.3	3.91; 81.1	6.61
12	121.1, 135.6, 163.4, 126.9, 92.1, 109.5 (dibenzofuran)	4.82; 98.2	5.45; 103.4	5.95
11	125.8, 120.0, 170.0, 120.0, 68.7, 117.7 (xanthone)	4.73; 90.5	4.77; 90.6	5.92
14	122.6, 159.8, 120.2, 123.2, 145.0, 103.3 (dibenzothiophene)	5.13; 110.2	6.24; 110.2	34.4

energy minimization of strain in **28**. The significant van der Waals interactions are assumed to involve, first, the interaction between the cysteine α-CH with the phenolic oxygen and the template S and, second, the transannular interactions of the cysteine α-CH, the NH, and the β-CH with the four nearest carbons and the oxygen atom of the dibenzofuran. Torsional and van der Waals potentials are defined as described by Allinger,[26,27] and neither bond distances nor bond angles are varied in this "soft" energy calculation. As described in the Appendix, a novel null-vector algorithm is used to define linear combinations of torsional motions at the six bonds B–G. These motions permit flexing of the cysteine backbone under the constraint of attachment to the rigid dibenzofuran template. The calculated energy minimum is a shallow trough in a broad valley where van der Waals strain is reduced to a very small value at the expense of torsional strain, which is 99% of the total strain at the energy minimum. The final strain energy and torsional angle values are reported in Table V, and the resulting conformation is depicted in **29ab**. In this structure, the α-H···O distance is increased to 2.5 Å.

Also included in Table V are the results of energy minimizations for acyl transfer transition states for the three cognate templates, phenoxathiin, xanthone, and dibenzothiophene. By calculation, the strain energy in transition states formed from the dibenzofuran and xanthone are equal, while that of the phenoxathiin is 0.6 kcal/mol higher. The calculated value for the dibenzothiophene transition state is nearly an order of magnitude higher, consistent with the failure to demonstrate any intramolecular reactivity for **14**.

The similarity of three of the calculated strain values masks differences in the sources of instability. For xanthone and dibenzofuran, the major effect that determines the stable conformation is the transannular interaction between the α-CH and the heterocyclic oxygen atom, and this effect is significantly larger in the dibenzofuran case, owing to the more acute angle at oxygen (see structure **18**). Owing to the nonplanarity of the phenoxathiin template, the transannular strain in this case is dominated by the bulk of the four heteroaromatic carbons at sites 3, 4, 6, and 7, as well as by interactions of the α-CH with the phenolic O and template S_2. For dibenzothiophene, the extended template length stretches **23**, allowing little conformational freedom, which compounds the strain induced by the bulky heteroaromatic sulfur. For this energy-minimized conformation spanned by dibenzothiophene, the calculated strain energy is reduced by 75% if the van der Waals parameters of thiophene sulfur are replaced by those for oxygen.

Although the results of energy minimization are in qualitative accord with experiment and confirm the assumptions of the basic conformational model, the quantitative fit at this stage of refinement is not impressive. By calculation, relative to that for dibenzofuran, the strain energies of the transition states derived from the phenoxathiin and xanthone templates are +0.5 and 0.0 kcal/mol, respectively. The corresponding experimental values derived from the data of Table II are +2.3 and +1.3 kcal/mol. A likely source of calculational error is the van der Waals function for oxygen, which is assumed to have spherical symmetry. Very likely the effective oxygen radius is reduced for edgewise interactions of the type seen in **28** and **29**, implying an overestimation of strain for **11** and particularly for **12** and **14**. By taking the phenoxathiin calculation to be the most accurate and combining results from experiment and calculation, one concludes that the dibenzofuran-bridged transition state is strained by approximately +4 kcal/mol. Strain of this magnitude is also consistent with the high EM value observed for the conformationally flexible template **10**, which evidently samples the same patch of conformation space.

Summary and Prospects for Further Study. This first exercise in molecular modeling with tunable templates has left several fundamental questions unanswered. Conformation **22** is almost certainly similar in energy to **23** and therefore is a likely candidate for a successful template-bridging experiment. It is perhaps surprising that no intramolecular acyl transfer could be demonstrated for template J of Table I. The likely explanation involves the substantial van der Waals interactions that result from the flat morphology of this backbone conformation as well as the excessive flexibility of the *o*-triphenylene template. (A 10° change in bond angle at the *o*-phenylene junction results in a 1-Å change in O–S_2 distance.) Further efforts to achieve efficient intramolecular acyl transfer in this extended region of the C_1–C_2, O–S_2 plane are planned.

It is also surprising that our optimal rigid template that achieves an EM value of 5–10 M generates a transition state with at least 4 kcal/mol of strain. Translated into concentration, this value implies an EM of at least 4×10^3 that could be realized with a hypothetical strain-free template that samples the 4.8, 5.2 Å region of the C_1–C_2, O–S_2 plane. As previously noted, energy calculations of this type are very parameter-sensitive, and an empirical alternative for assessing the magnitude and nature of steric interaction in the transition state **28** involves synthesis and X-ray crystallographic structure assignment for a stable analogue. A likely candidate might be generated by replacing the ortho amide function of **28** by a cyclic urethane.

Rigid, nonplanar structures appear to be the most promising second-generation templates for exploring the 4.8, 5.2 Å region while reducing van der Waals strain. A 1,9-difunctionalized phenoxathiin is a likely candidate, since it should share the small van der Waals destabilization of **13** and the O–S_2 distance of **12**. Work with this system is in progress.

It is clear that EM values at least in the hundreds and probably in the thousands can be expected for the reaction **1** → **3** when bridged by properly designed band-like templates, and that this reaction can doubtless be elevated to the EM range of S_N2 substitutions seen with small molecules such as **4** and **5** or, equivalently, to the range of the surface-sited disulfide bond formation of reduced BPTI studied by Creighton and Goldenberg.[8] More refined studies will be required to determine whether band-like templates are capable of generating significantly larger EM values for reactions that proceed via medium-sized rings. The cleanness and speed of enzymatically catalyzed reactions are usually attributed to a three-dimensional complementarity between substrate and enzyme

in which surfaces more tailored and intricate than bands undergo intimate van der Waals interactions at the active site. Extensions of the present studies may permit sharpening of our present sense of the necessity of sizeable tailored contact and the degree to which optimally designed templates that act merely as bands can approximate the catalytic efficiency of enzymes.

Experimental Section

IR spectra were recorded on a Perkin-Elmer Model 283-B spectrometer. High-resolution ^1H NMR spectra were obtained on either a Bruker WM-250 or a Bruker WM-270 instrument. Chemical shifts are reported in parts per million downfield from tetramethylsilane, and splitting patterns are designated as s, singlet; d, doublet; t, triplet; q, quartet; m, multiplet; br, broad: and d of m, doublet of multiplets; only major peaks are reported for peptide spectra. Coupling constants are given in hertz. Low-resolution, high-resolution, and field-desorption mass spectra were recorded on Varian MAT-44, CEC-110, and Finnigan MAT-731 mass spectrometers, respectively. Microanalyses were performed by Galbraith Laboratories, Knoxville, TN.

Analytical thin-layer chromatography was performed on glass precoated silica gel 60 plates (Merck F-254). Preparative layer chromatography was performed on Analtech GF plates, and flash chromatography was carried out on silica gel 60 (230–400 mesh) using 100% dichloromethane as eluent. HPLC was performed on a Waters system consisting of two Model 6000-A pumps, a Model 680 automated gradient controller, a Model U6K injector, a Model 440 dual-channel UV detector (280, 254 nm), and a Model 730 data module. HPLC runs were conducted in the reverse-phase mode on Whatman Partisil columns. Unless otherwise specified, chemicals were reagent grade. (Methoxycarbonyl)sulfenyl chloride was prepared by literature procedures[29] and purified by careful spinning-band distillation.

Methyl *S*-[[[2-[(Benzyloxycarbonyl)-L-alanyloxy]-5-chlorophenyl]methyl]thio]-L-cysteinate (8). A. 2-Hydroxy-5-chlorobenzyl Alcohol. A solution of 10 g (58 mmol) of 5-chlorosalicylic acid in 100 mL of anhydrous ether was added dropwise with stirring under N_2 to a solution of 3.29 g (900 mmol) of lithium aluminum hydride in 100 mL of ether. After the addition was complete, the mixture was maintained at reflux for 45 min and then was treated cautiously with water and with 200 mL of 10% sulfuric acid. The aqueous phase was separated and reextracted, and the pooled ether layers were washed, dried ($MgSO_4$), and evaporated to give a solid, which was recrystallized from chloroform to yield 8.9 g (97%) of the title compound, mp 90–91.5 °C.

B. 2-[[(Methoxycarbonyl)dithio]methyl]-4-chlorophenol. To a solution of 40 g (25 mmol) of 2-hydroxy-5-chlorobenzyl alcohol in 10 mL of pyridine was added 9.7 mL of acetic anhydride. After 2 h at 25 °C, the volatiles were evaporated, and the resulting oil was taken up in CH_2Cl_2, washed with 1 M HCl, water, and brine, then dried, and stripped of CH_2Cl_2 to give 5.9 g (97%) of 2-acetoxy-5-chlorobenzyl acetate as an oil: ^1H NMR (250 MHz, $CDCl_3$) 2.10 (s, 3 H), 2.34 (s, 3 H), 5.06 (s, 2 H), 7.04 (d, 1 H), 7.37 (d, 1 H), 7.42 (s, 1 H).

To 2.0 g (8.3 mmol) of the above diacetate was added a solution of 1.9 g of sodium hydrogen sulfide in 50 mL of methanol, prepared by saturating a solution of sodium methoxide in methanol with hydrogen sulfide. The mixture was heated to reflux for 2 h, then cooled, and evaporated. Water and CH_2Cl_2 were added, the layers were separated, and the CH_2Cl_2 layer was washed, dried, and evaporated to give 1.3 g (91%) of 2-hydroxy-5-chlorobenzyl mercaptan as a colorless oil. The thiol (1.32 g, 7.5 mmol) was dissolved in 10 mL of 1:1 chloroform–methanol and treated dropwise with 0.7 mL (7.6 mmol) of (methoxycarbonyl)sulfenyl chloride.[29] After 24 h at 25 °C, the solvent was evaporated, and the residue was purified by preparative layer chromatography on silica (9:1 chloroform–ethyl acetate) to give crystalline cubes of the title compound: 1.34 g (67%); mp 110–111.5 °C; ^1H NMR (60 MHz, $CDCl_3$) 3.97 (s, 3 H), 4.02 (s, 2 H), 6.82–7.30 (m, 4 H).

Anal. Calcd for C_9H_9ClOS: C, 40.83; H, 3.43; Cl, 13.39; S, 24.22. Found: C, 41.07; H, 3.42; Cl, 13.57; S, 23.99.

C. Methyl *S*-[[[2-[(Benzyloxycarbonyl)-L-alanyloxy]-5-chlorophenyl]methyl]thio]-L-cysteinate Hydrochloride (8·HCl). To a solution of 0.32 g (1.21 mmol) of the Scm derivative prepared in step B in 11 mL of methanol was added 0.3 g (1.28 mmol) of methyl *N*-(*tert*-butoxycarbonyl)-L-cysteinate. After 90 min at 25 °C, the solvent was evaporated, and the residue was purified by preparative layer chromatography on silica (9:1 dichloromethane–ethyl acetate) to give 0.21 g (43%) of the unsymmetrical cysteine disulfide. A solution of this substance in 1 mL of ethyl acetate was added to a mixed carbonic–carboxylic anhydride formed by combining 123 mg (0.50 mmol) of Z-L-Ala-OH, 81 μL of triethylamine, and 72 μL of isobutyl chloroformate in 2 mL of ethyl acetate at −12 °C. After 15 h at −12 °C, the solvent was evaporated, and the residue was taken up in dichloromethane, washed with 0.5 M citric acid, 5% $NaHCO_3$, water, and brine, dried, and evaporated. The gummy product was purified by preparative layer chromatography on silica (9:1 dichloromethane–ethyl acetate) to give 0.20 g (63%) of an oil, which was treated with 2 mL of dioxane, freshly saturated with dry HCl. The solution was frozen in liquid nitrogen and allowed to thaw and evaporate in vacuum. Trituration with anhydrous ether gave an amorphous white solid, 16 mg (89%), mp 151–153 °C, of the title compound: ^1H NMR (250 MHz, $CDCl_3$, as free base) 1.55 (d, 3 H), 1.70 (br s, 2 H), 2.80 (dd, 2 H), 3.72 (s, 3 H), 3.80 (s, 2 H), 4.4–4.8 (m, 2 H), 5.20 (s, 2 H), 5.60 (m, 2 H), 7.0–7.35 (m, 3 H), 7.40 (s, 5 H).

Anal. Calcd for $C_{22}H_{26}N_2Cl_2O_6S_2$: C, 48.09; H, 4.77; S, 11.67. Found: C, 47.92; H, 4.96; S, 11.76.

D. O,N-Acyl Transfer with 8. Methyl *N*-(Benzyloxycarbonyl)-L-alanyl-L-cysteinate and Methyl *N*-(Benzyloxycarbonyl)-L-alanyl-*S*-(2-hydroxy-5-chlorobenzyl)-L-cysteinate. The HCl salt prepared in step C (21.9 mg, 0.040 mmol) was partitioned between ice-cold 5% $NaHCO_3$ and $CHCl_3$. The $CHCl_3$ was evaporated from the dried organic phase, and the residue was taken up in 100 mL of freshly distilled DMSO (concentration, ca. 4×10^{-4} M) and stirred for 44 h. The DMSO was evaporated, and the residue was dissolved in 0.2 mL of methanol containing 8 mg of dithiothreitol. After 2 h, the mixture was diluted with CH_2Cl_2, washed with water and brine, and then dried. The CH_2Cl_2 was evaporated, and preparative layer chromatography (9:1 dichloromethane–ether) gave 3 mg (22%) of Z-L-Ala-L-Cys-OMe and 9.4 mg (47%) of Z-L-Ala-L-Cys(2-HO-5-Cl-Bzl)-OMe, each identified by comparison with an authentic sample, synthesized as described below. The latter compound is doubtless formed as the result of a sulfur extrusion from and $R-S_2^-$ species, formed by a reversible fragmentation of the *o*-hydroxybenzyl function; extensive disulfide interchange accompanies the slow acyl transfer reaction.

Z-L-Ala-L-Cys-OMe was prepared by mixed anhydride acylation of dimethyl LL-cystinate, followed by dithiothreitol cleavage: white needles from ether–pentane, mp 114–115 °C.

Anal. Calcd for $C_{15}H_{20}N_2O_5S$: C, 52.93; H, 5.92; N, 8.23; S, 9.42. Found: C, 52.70; H, 6.12; N, 8.27; S, 9.58.

Z-L-Ala-L-Cys(2-HO-5-Cl-Bzl)-OMe was prepared by reaction of 2-hydroxy-5-chlorobenzyl bromide, mp 98–99 °C, with the above peptide in chloroform in the presence of 1 equiv of triethylamine: crystals from chloroform, mp 140–141 °C.

Anal. Calcd for $C_{22}H_{25}N_2ClO_6S$: C, 54.94; H, 5.24; S, 6.67. Found: C, 54.91; H, 5.53; S, 6.56.

E. Estimation of an EM Value for the Intramolecular O,N-Acyl Transfer of 8. From a series of experiments of the type described in step D, the half-life for the intramolecular O,N-acyl transfer reaction of **9** can be estimated to lie in the range of 10–40 h, which corresponds to a first-order rate constant of $(0.5–2) \times 10^{-5}$ s^{-1}. From models (see later discussion), the rate constant for a corresponding intermolecular reaction probably lies in the range of $(2–10) \times 10^{-6}$ M^{-1} s^{-1}, and the range of EM values is therefore 0.5–10 M.

Methyl *S*-[[2-[(Benzyloxycarbonyl)-L-alanyloxy]-phenyl]thio]-L-cysteinate (9). A. 2-[(Methoxycarbonyl)-dithio]phenol. A solution of 2.1 g (16.7 mmol) of *o*-mercaptophenol, prepared by the procedure of Djerassi et al.,[30] in 18 mL

(29) Weiss, W. Ger. Pat. 1223720, Farbenfabriken Bayer A.G., 1966. Zupancic, B. *Synthesis* **1975**, 169.

of methanol was cooled to −10 °C and treated with 1.6 mL of (methoxycarbonyl)sulfenyl chloride. After 2 h, the mixture was warmed to 25 °C and chromatographed on silica gel, eluting with chloroform to yield 2.5 g (69%) of product as a pale green oil: ^{1}H NMR (60 MHz, $CDCl_3$) 4.00 (s, 3 H), 6.8–7.8 (m, 4 H), 8.35 (s, 1 H).

B. Methyl *N*-(*tert*-Butoxycarbonyl)-*S*-[[2-[(benzyloxycarbonyl)-L-alanyloxy]phenyl]thio]-L-cysteinate. The title compound was prepared in two steps from the *o*-(Scm-S)-phenol formed in step A. A solution of 0.21 g (0.95 mmol) of the product of step A and 0.25 g (1.1 mmol) of Boc-L-Cys-OMe in 10 mL of 1:1 chloroform–methanol was stripped of solvent after 2 h at 25 °C, and the residue was purified by preparative layer chromatography (9:1 dichloromethane–ethyl acetate) to give methyl *S*-[(2-hydroxyphenyl)thio]-L-cysteinate as an oil, 0.25 g, 68%. A solution of 0.059 g (0.17 mol) of the above product in 0.4 mL of ethyl acetate was added to the mixed anhydride prepared by combining 40.6 mg (0.18 mmol) of Z-L-Ala-OH, 28 μL of triethylamine, and 24 μL of isobutyl chloroformate in 0.6 mL of ethyl acetate at −12 °C. The mixture was stirred overnight at −12 °C, the solvent evaporated, and the residue taken up in dichloromethane, washed with 0.5 M citric acid, 5% $NaHCO_3$, water, and brine, and dried. Evaporation of CH_2Cl_2 followed by preparative layer chromatography on silica (9:1 dichloromethane–ethyl acetate) gave an oil, which was crystallized from ether–pentane: 47 mg, 51%; mp 83–84 °C; ^{1}H NMR (250 MHz, $CDCl_3$) 1.40 (s, 9 H), 1.65 (d, 3 H), 3.10 (m, 2 H), 3.68 (s, 3 H), 4.60 (m, 2 H), 5.12 (m, 3 H), 5.50 (m, 1 H), 7.30 (br s, 9 H), 7.70 (m, 1 H); high-resolution mass spectrum calcd 564.1600, found 564.1610.

Anal. Calcd for $C_{26}H_{32}N_2O_8S_2$: C, 55.30; H, 5.71; N, 4.96; S, 11.36. Found: C, 55.41; H, 5.86; N, 4.94; S, 11.23.

C. Methyl *S*-[[2-[(Benzyloxycarbonyl)-L-alanyloxy]-phenyl]thio]-L-cysteinate Hydrochloride (9·HCl) and O,N-Acyl Transfer Experiments with 9. The *N*-Boc derivative prepared in step B was treated with dioxane freshly saturated with HCl for 30 min at 25 °C; the solution was then frozen in liquid nitrogen and allowed to thaw under high vacuum. Trituration of the residue with ether gave 91% of the hydrochloride salt of **9**. In a typical acyl transfer experiment, 15.4 mg (0.027 mmol) of this salt was dissolved in 0.35 mL of DMSO and treated with 4.5 μL of triethylamine (1 equiv). After 24 h, the solvent was evaporated, and the residue was taken up in dichloromethane, washed with water and brine, then dried, and evaporated to an oil, which was dissolved in 0.2 mL of methanol and treated with 11 mg of dithiothreitol for 3 h at 25 °C. Dichloromethane was added, and the solution was washed with water and brine, then dried, and evaporated. The residual oil was purified by preparative layer chromatography (9:1 dichloromethane–ether), which gave 3 mg, 25%, of Z-L-Ala-L-Cys-OMe, identical in all respects with an authentic sample. An isotopic dilution experiment using **9** labeled with ^{14}C in the alanine function gave a yield of 50% for the peptide.

D. Estimation of an EM Value for the O,N-Acyl Transfer Reaction of 9. Yields of dipeptide from experiments described in step C were invariant to substrate concentration over the range of (1–4) × 10^{-4} M, and although competing disulfide interchange and other redox chemistry complicated the product mixture and made interpretation of kinetics difficult, ^{1}H NMR spectra of the reaction mixture and the results of quenching at specific times and product assay by isotopic dilution set bounds on the rate constant for intramolecular acyl transfer of (0.4–2.5) × 10^{-5} s^{-1}. From model compounds (see below), the rate constant for the corresponding intermolecular acyl transfer reaction can be estimated to lie in the range of (2–5) × 10^{-5} M^{-1} s^{-1}, from which the EM can be estimated to lie in the range of 0.08–1.3 M.

Ethyl *S*-[[(4-Acetoxy-5-xanthenyl)methyl]thio]-L-cysteinate (10). A. 4-Hydroxy-5-(hydroxymethyl)xanthene. To a solution in 10 mL of ethanol of 107 mg (0.473 mmol) of 4-hydroxy-5-formylxanthene, prepared as previously reported,[3] was added 36 mg (0.92 mmol) of sodium borohydride. After 1.3 h, the solution was poured into 50 mL of 1 M HCl and extracted with CH_2Cl_2. The extracts were washed, dried ($MgSO_4$), and concentrated to give 105 mg, 97%, of the title compound: mp 138.5–139 °C; ^{1}H NMR (250 MHz, Me_2CO-d_6) 3.93 (s, 2 H), 4.55 (br s, 1 H), 4.86 (s, 2 H), 6.5–7.4 (m, 6 H), 8.00 (br s, 1 H).

Anal. Calcd for $C_{14}H_{12}O$: C, 73.67; H, 5.30. Found: C, 73.34; H, 5.33.

B. Ethyl *N*-(*tert*-Butoxycarbonyl)-*S*-[[(4-acetoxy-5-xanthenyl)methyl]thio]-L-cysteinate. A solution of 54 mg (0.24 mmol) of 4-hydroxy-5-(hydroxymethyl)xanthene in 10 mL of ethanol was treated with a vigorous stream of HBr for 1 min, then heated to reflux for 30 min, and poured into ice–water. The organic phases from extraction with CH_2Cl_2 were pooled, washed with 5% $NaHCO_3$, dried, and evaporated, and the residue was dissolved in a minimum of ethanol and added to a solution prepared by dissolving 15 mg of NaH (0.63 mmol) in 10 mL of ethanol and saturating the solution with H_2S. The resulting solution was stirred at reflux under H_2S for 2 h, cooled, poured into 50 mL of 1 M HCl, and extracted with CH_2Cl_2. The dried CH_2Cl_2 phases were evaporated, and the residue was taken up in 10 mL of methanol containing 22 μL of (methoxycarbonyl)-sulfenyl chloride. After 15 min, the solvent was evaporated, and the residue was purified by preparative layer chromatography (9:1 chloroform–ethyl acetate) to give 27 mg, 34%, of 4-hydroxy-5-[[(methoxycarbonyl)dithio]methyl]xanthene, mp 116–118 °C. A solution of 66 mg (0.20 mmol) of this substance in 2 mL of pyridine containing 0.20 mL of acetic anhydride was stirred for 40 min, then poured into 1 M HCl, and extracted with CH_2Cl_2. The CH_2Cl_2 phase was washed, dried, and evaporated to give 61 mg, 83%, of 4-acetoxy-5-[[(methoxycarbonyl)dithio]methyl]xanthene as an oil: ^{1}H NMR (250 MHz, $CDCl_3$) 2.44 (s, 3 H), 3.80 (s, 3 H), 4.06 (s, 4 H), 7.05 (m, 6 H).

To a solution of 45 mg (0.12 mmol) of the above compound in 4 mL of 1:1 chloroform–methanol was added 30 mg (0.12 mmol) of Boc-L-Cys-OEt and 17 μL of triethylamine (0.12 mmol). After 2 h at 25 °C, the solution was poured into a mixture of ice-cold 1 M HCl and dichloromethane. The combined organic extracts were washed, dried ($MgSO_4$), and evaporated to give 65 mg (97%) of the title compound as an oil: ^{1}H NMR (250 MHz, $CDCl_3$) 1.15 (t, 3 H, J = 7), 1.40 (s, 9 H), 2.40 (s, 3 H), 2.90 and 3.13 (2 d, 2 H, J = 5), 3.97 (s, 2 H), 4.02 (s, 2 H), 4.10 (q, 2 H, J = 7), 4.27 (m, 1 H), 5.30 (br s, 1 H), 7.00 (m, 6 H).

C. Preparation of the HCl Salt of 10 and the O,N-Acyl Transfer Reaction of 10. A solution in dioxane freshly saturated with HCl of the Boc derivative prepared in step B was stirred at 25 °C for 20 min and then evaporated. The residue was triturated with hexane and used directly in acyl transfer experiments. The O,N-acyl transfer reaction was followed either by ^{1}H NMR spectroscopy at ca. 0.09 M or by UV spectroscopy at (1–2) × 10^{-4} M. In the latter case, a stock solution of the hydrochloride in DMSO or DMF was diluted to the appropriate concentration and treated with 10 equiv of triethylamine. The rate of reaction was followed at 282 nm, 25 °C, for three or four half-lives. The half-life for the NMR experiment was defined to be the point at which areas of acetyl resonances for starting material and product were equal. Rate constants by UV and NMR methods were equal within experimental error, establishing the acyl transfer reaction to be intramolecular. Thin-layer and HPLC examination of the product mixture from the NMR experiments revealed the presence of ethyl *N*-acetoxy-*S*-[[(4-hydroxy-5-xanthenyl)methyl]thio]-L-cysteinate, confirmed by independent synthesis, as well as the products of disulfide interchange.

D. Calculation of an EM Value for the O,N-Acyl Transfer Reaction of 10. The rate constant for the intramolecular acyl transfer reaction of **10** in DMSO at 25 °C is (1.0–1.4) × 10^{-5} s^{-1}; estimates (see below) for the rate constant for the corresponding intermolecular reaction lie in the range of (1–3) × 10^{-6} M^{-1} s^{-1}. The EM value therefore lies in the range of 3–14 M.

Ethyl *S*-[(1,5-Diacetoxy-3-methoxy-2-methyl-9-oxo-9*H*-xanthen-4-yl)thio]-L-cysteinate (11). A. Bis(1,5-dihydroxy-3-methoxy-2-methyl-9-oxo-9*H*-xanthen-4-yl) Sulfide. The title compound was prepared by electrophilic sulfenation of 1,5-dihydroxy-3-methoxy-2-methylxanthone, obtained by following the general procedure of Shah.[31] A mixture of 15

(30) Djerassi, C.; Gorman, M.; Markley, F.; Oldenberg, E. *J. Am. Chem. Soc.* **1955**, *77*, 568.

(31) Dalal, S.; Shah, R. *Chem. Ind. (London)* **1957**, 140. Bose, J.; Shah, R. *J. Indian Chem. Soc.* **1961**, *38*, 701.

g (97 mmol) of 2,3-dihydroxybenzoic acid, 15 g (89 mmol) of 2-methyl-3,5-dimethoxyphenol, 50 g (0.37 mol) of fused zinc chloride, and 100 mL of phosphorus oxychloride was stirred at 75 °C for 2 h, then poured hot onto 700 g of ice, and swirled vigorously for 3 min. After 1 h, the precipitate was collected on a large Büchner funnel and washed with saturated sodium bicarbonate solution. Recrystallization from methanol gave 2.28 g (9.5%) of 1,5-dihydroxy-3-methoxy-2-methylxanthone, mp 165–170 °C. The compound gave the green color with ferric chloride that is characteristic of 1-hydroxyxanthones: ^{1}H NMR (250 MHz, DMSO-d_6) 2.00 (s, 3 H), 3.97 (s, 3 H), 6.75 (s, 1 H), 7.35 (m, 2 H), 7.65 (dd, 1 H, J = 4, 6), 10.3 (br s, 1 H), 12.9 (s, 1 H).

To a suspension of 172 mg (0.630 mmol) of the above compound in 3 mL of chloroform at 0 °C was added 0.04 mL (0.42 mmol) of sulfur monochloride and 25 mg of aluminum chloride. The resulting mixture was stirred for 6 h and then was evaporated, and the residue was gently warmed and stirred in 20 mL of methanol. After 4 h at 5 °C, 140 mg (77%) of yellow solid was collected: mp 339–340 °C; ^{1}H NMR (250 MHz, DMSO-d_6) 2.09 (s, 3 H), 3.88 (s, 3 H) 7.28 (m, 2 H), 7.59 (m, 1 H), 10.22 (s, 1 H), 13.28 (s, 1 H); mass spectrum (70 eV), m/e 574 (M^+, 1.61), 573 (29.2), 303 (11.0), 273 (12.4), 242 (9.6), 109 (16.7), 69 (61), 57 (84), 43 (100).

Anal. Calcd for $C_{30}H_{22}O_{10}S$: C, 62.71; H, 3.86; S, 5.58. Found: C, 62.91; H, 3.91; S, 5.31.

B. 1,5-Dihydroxy-3-methoxy-2-methyl-4-[(methoxycarbonyl)dithio]xanthone. A solution of 1.3 g of the crude product obtained as described in step A was heated to reflux for 1 h in a mixture of 12 mL of 1 M NaOH and 0.5 g (2.1 mmol) of disodium sulfide nonahydrate. The cooled solution was poured into 50 mL of 1 M HCl, and the precipitated solid was filtered, washed with water, dried in vacuum, and dissolved in 300 mL of hot methanol. To the cooled solution was added 0.36 mL (3.9 mmol) of (methoxycarbonyl)sulfenyl chloride. After 30 min, the solution was evaporatively absorbed onto 5 g of silica gel, which was then added to the top of a 50-g silica gel column. Elution with chloroform gave 0.51 g (33%) of the title compound, recrystallizable from ether: mp 181–182 °C; ^{1}H NMR (250 MHz, $CDCl_3$) 2.21 (s, 3 H), 3.87 (s, 3 H), 3.94 (s, 3 H), 7.38 (m, 2 H), 7.76 (dd, 1 H, J = 2,6), 8.00 (br s, 1 H), 13.60 (s, 1 H); mass spectrum (70 eV), m/e (relative intensity) 394 (M^+, 25), 303 (100), 288 (8), 241 (21), 136 (30), 69 (41), 43 (41).

Anal. Calcd for $C_{17}H_{14}O_7S_2$: C, 51.77; H, 3.58; S, 16.26. Found: C, 51.84; H, 3.60; S, 16.05.

C. Ethyl *N*-(*tert*-Butoxycarbonyl)-*S*-[(1,5-diacetoxy-3-methoxy-2-methyl-9-oxo-9*H*-xanthen-4-yl)thio]-L-cysteinate. Numerous attempts to generate this unsymmetrical disulfide by Scm chemistry failed. The substance was generated in three steps from compound B. A solution of 1.21 g (4.45 mmol) of the compound prepared in B, 7.5 mL (8.0 mmol) of acetic anhydride, and 7.5 mL of pyridine was stirred at 25 °C for 1 h, then poured into 100 mL of 1 M HCl and 100 mL of CH_2Cl_2. The combined CH_2Cl_2 extracts were washed with water, dried ($MgSO_4$), and evaporated to give 1.42 g (100%) of the 1,5-diacetoxy derivative, mp 129–134 °C. To a solution of 31 mg (0.04 mmol) of this substance in 7 mL of $CHCl_3$ was added 7 mg (0.045 mmol) of dithiothreitol, 1 drop of water, and 1 drop of triethylamine. After 1 h of stirring at 25 °C, the solution was extracted with 10 mL of 1 M HCl and dried. Evaporation of the $CHCl_3$ gave 30 mg (97%) of 1,5-diacetoxy-4-mercapto-3-methoxy-2-methylxanthone, mp 199–202 °C, which was used immediately in the following oxidation experiment.

To a solution of 29 mg (0.075 mmol) of the above thiol in 2 mL of chloroform containing 0.19 g (0.76 mmol) of Boc-L-Cys-OEt was added dropwise over 4 min 0.22 g (0.87 mmol) of iodine in 5 mL of chloroform. After 1 h of stirring at 25 °C, the solution was diluted with CH_2Cl_2 and washed with freshly prepared 5% aqueous ascorbic acid and with water. The residue obtained after drying and evaporation of CH_2Cl_2 was purified by preparative layer chromatography (ether). The second-highest band contained the title compound, 14 mg, 30%, isolated as an oil: ^{1}H NMR (250 MHz, $CDCl_3$) 1.10 (t, 3 H, J = 7), 2.20 (s, 3 H), 2.50 (s, 6 H), 3.16 (d, 2 H, J = 6), 3.96 (s, 3 H), 4.18 (q, 2 H, J = 7), 4.68 (m, 1 H), 5.30 (br d, 1 H), 3.96 (s, 3 H), 4.18 (q, 2 H, J = 7), 4.68 (m, 1 H), 5.30 (br d, 1 H), 7.40 (m, 2 H), 8.07 (br d, 1 H, J = 7).

D. Preparation of the Hydrochloride Salt of 11. O,N-Acyl Transfer Reaction of 11. To a solution of 12 mg (0.020 mmol) of the Boc derivative prepared in step C was added 2 mL of HCl-saturated dioxane. After 45 min at 25 °C, the solution was frozen and lyophilized. The residue was triturated with ether–hexane to give 5 mg of the HCl salt of **11**, 50%, mp 162–165 °C, which was used directly in acyl transfer reactions. Reaction kinetics were followed as described for **10**; the UV kinetics were strictly linear for the first 25 h of the reaction. First-order rate constants in DMSO and DMF at 25 °C of 7.0×10^{-5} and 6.8×10^{-6} M^{-1} s^{-1}, respectively, were observed. The second-order rate constants for the analogous intermolecular reactions in DMSO and DMF can be estimated at 1.2×10^{-4} and $(0.9–1.2) \times 10^{-5}$ M^{-1} s^{-1}, respectively (see below). Consequently, the EM for the intramolecular reaction is in the range of 0.5–0.7 M.

Methyl *S*-[(6-Acetoxy-4-dibenzothiophene-yl)thio]-L-cysteinate (14). A. 6-Methoxy-4-mercaptodibenzothiophene. This substance was prepared in low yield from the lithiation product of 6-methoxydibenzothiophene, in turn prepared from dibenzothiophene. The route parallels the synthesis of the corresponding dibenzofuran derivative.[1] The structure of the final product follows from its ^{1}H NMR spectrum.

1. 4-Hydroxydibenzothiophene and 4-Acetoxydibenzothiophene. To a solution of 166 g (0.90 mol) of dibenzothiophene in 1.8 L of ether was added slowly at 25 °C (400 mL (0.92 mol) of butyllithium in hexane. The resulting dark orange solution was heated to reflux for 20 h and then cooled to −30 °C as O_2 was bubbled through for 1 h. To the milky suspension was added by cannula 0.90 mol of 2.85 M ethylmagnesium bromide in ether was continuing flow of O_2 at −10 to −30 °C. The mixture was maintained at that temperature for an additional 1.5 h and then was warmed to 25 °C overnight. Sufficient 6 M HCl was added to achieve a good phase separation, the layers were separated, and the aqueous phase was reextracted. The pooled ether phases were washed with water and 1 M HCl and then extracted with 4 × 100 mL of 1 M NaOH. The basic extracts were pooled, washed with ether, cooled, and acidified to pH 1 with HCl, giving a suspension, which was extracted with CH_2Cl_2. The pooled extracts were washed with water, dried, and concentrated to yield 83.8 g, 43.6%, of a tan-brown solid that was purified by Kugelrohr distillation at 110 °C and recrystallization from methanol–water to give needles: 72.1 g, 40%; mp 165–166 °C; ^{1}H NMR (250 MHz, $CDCl_3$) 5.40 (s, 1 H), 6.88 (d, 1 H, J = 8, C_3-H), 7.33 (t, 1 H, J = 8, C_2-H), 7.46 (m, 2 H, $C_{7,8}$-H), 7.78 (d, 1 H, J = 8, C_1-H), 7.89 (m, 1 H, C_6-H), 8.13 (m, 1 H, C_9-H).

Acetylation of the product with acetic anhydride containing a drop of H_2SO_4, followed by aqueous workup and recrystallization from ethanol, gave 4-acetoxydibenzothiophene, 75%, mp 98 °C.

2. 4-Methoxydibenzothiophene. To a mixture of 69.2 g (0.345 mmol) of crude 4-hydroxydibenzothiophene and 71 g (0.52 mmol) of K_2CO_3 in 2.4 L of acetone at 40 °C was added slowly with stirring 500 g (3.52 mol) of methyl iodide. The suspension was heated to reflux with stirring for 20 h, then cooled, filtered, and evaporated. The residue was dissolved in a mixture of equal volumes of CH_2Cl_2 and water, and the aqueous layer was reextracted. The pooled organic layers were washed with 50 mL of 1 M NaOH, water, and brine, then dried, and concentrated. The residue was recrystallized from ethanol to give long white needles: 55 g, 75%; mp 122–123 °C; ^{1}H NMR (250 MHz, $CDCl_3$) 4.04 (s, 3 H), 6.98 (d, 1 H, J = 8, C_3-H), 7.42 (m, 3 H, $C_{2,7,8}$-H), 7.78 (d of m, 1 H, J = 8, C_1-H), 7.87 (d of m, 1 H, J = 8, C_6-H), 8.13 (d of m, 1 H, J = 8, C_9-H).

3. 4-Methoxy-6-mercaptodibenzothiophene. To a solution of 10 g (0.047 mol) of 4-methoxydibenzothiophene in 125 mL of freshly distilled tetrahydrofuran at −30 °C was added with stirring under N_2 25 mL (0.05 mol) of *n*-butyllithium in hexane. The resulting bright yellow mixture was stirred at −25 °C for 3.5 h, at which time 1.60 g (0.050 mol) of elemental sulfur was added in one portion. This mixture was allowed to warm to room temperature slowly (ca. 3 h), yielding a clear yellow solution, which was carefully acidified at 0 °C with 10% HCl and then poured into ice-cold 10% HCl. This acidic solution was extracted with ethyl ether (4×). The ether layers were combined, washed with water (1×), and extracted with 0.5 N NaOH (4×). The basic layers were combined, washed with ether (3×), and acidified to pH 1 with concentrated HCl, yielding a milky, yellowing suspension,

which was extracted with CH_2Cl_2 (4×). The organic layers were combined, washed with water (2×) and brine (1×), dried with $MgSO_4$, filtered, and concentrated to a yellow oil possessing a strong thiol odor. This oil was passed through a plug of silica gel via vacuum with a 3:1 hexanes–ethyl acetate eluent, leaving an odorless pale yellow solid. Two recrystallizations from CH_2Cl_2–pentane gave small pale yellow crystals of pure 4,6-disubstituted product free from other regioisomers: 380 mg, 3.3%; mp 143 °C; ^1H NMR (250 MHz, $CDCl_3$) 3.67 (s, 1 H), 4.04 (s, 1 H), 6.93 (d, 1 H, J = 8, C_3-H), 7.40 (m, 2 H, $C_{2,8}$-H), 7.73 (d, 1 H, J = 8 Hz, C_1-H), 7.85 (d of m, 1 H, J = 8, C_7-H), 7.98 (d, 1 H, J = 8, C_9-H); mass spectrum (70 eV), m/e (relative intensity) 246 (M^+, 100), 231 (40), 203 (39), 171 (11), 158 (19).

Anal. Calcd for $C_{13}H_{10}OS_2$: C, 63.38; H, 4.10. Found: C, 63.09; H, 4.16.

B. 4-Mercapto-6-hydroxydibenzothiophene, 4-[(Methoxycarbonyl)dithio]-6-hydroxydibenzothiophene, and 4-[(Methoxycarbonyl)dithio]-6-acetoxydibenzothiophene. To a solution of 357 mg (1.45 mmol) of 4-mercapto-6-methoxydibenzothiophene in 4.5 mL of dry $CHCl_3$ was added in one portion at 25 °C under N_2 1.05 mL (7.3 mmol) of trimethylsilyl iodide. This mixture was heated to reflux for 48 h, and the resulting dark red solution was cooled to 25 °C, poured into 30 mL of methanol, and stirred. This partially decolorized solution was evaporated to a dark red oil, which was taken into 70 mL of 1:1 CH_2Cl_2–water. The water layer was separated and reextracted, and the combined organic layers were washed with 10% Na_2SO_3 (2×), water, and brine, dried over $MgSO_4$, filtered, and concentrated to give 208 mg of 4-mercapto-6-hydroxydibenzothiophene, 62%, as a pale yellow powder. Recrystallization from CH_2Cl_2 at −20 °C yielded a pale yellow, odorless, fluffy solid: mp 161–162 °C; ^1H NMR (250 MHz, $CDCl_3$) 3.68 (s, 1 H), 5.35 (s, 1 H), 6.91 (d, 1 H, J = 8, C_3-H), 7.36–7.52 (m, 3 H), 7.75 (d, 1 H, J = 8, C_1-H), 8.01 (d, 1 H, J = 8, C_9-H).

To a solution of 65 mg (0.28 mmol) of 4-mercapto-6-hydroxydibenzothiophene in 1 mL of methanol at 25 °C was added with vigorous stirring under N_2 30 μL (0.33 mmol) of (methoxycarbonyl)sulfenyl chloride. After 30 min, the solvent was evaporated to yield a pale yellow solid, which was dried by azeotropic distillation with CH_3CN (2×), then dissolved in CH_2Cl_2, passed through a silica gel plug, and evaporated to yield 85.1 mg, 94%, of 4-[(methoxycarbonyl)dithio]-6-hydroxydibenzothiophene as a pale yellow solid: mass spectrum (70 eV), m/e (relative intensity) 322 (M^+, 78.3), 263 (68.1), 231 (100), 214 (32.4), 203 (22), 187 (45.8), 171 (40.5), 158 (26.2), 59.1 (21.9).

A solution of 36 mg (0.11 mmol) of the above solid in 0.75 mL of $CHCl_3$ and 1.5 mL of acetic anhydride was treated with 6 μL of H_2SO_4, stirred under N_2 for 2 h, then poured into 5% $NaHCO_3$–ice, and extracted with dichloromethane (4×). The organic layers were combined, washed with 5% $NaHCO_3$ (3×), water (1×), and brine (1×), dried over $MgSO_4$, filtered, and evaporated to yield 36 mg, 89%, of 4-[(methoxycarbonyl)dithio]-6-acetoxydibenzothiophene as a pale yellow gum: ^1H NMR (250 MHz, $CDCl_3$) 2.48 (s, 3 H), 3.91 (s, 3 H), 7.34 (d, 1 H, J = 8, C_3-H), 7.50 (t, 1 H, J = 8, C_2-H), 7.52 (t, 1 H, J = 8, C_8-H), 7.89 (d, 1 H, J = 8, C_7-H), 8.02 (d, 1 H, J = 8, C_1-H), 8.15 (d, 1 H, J = 8, C_9-H); mass spectrum (70 eV), m/e (relative intensity) 364 (M^+, 77), 322 (99), 278 (32), 263 (100), 231 (100), 214 (35), 187 (30), 171 (21), 158 (28), 203 (19).

C. Methyl *N*-(*tert*-Butoxycarbonyl)-*S*-[(6-acetoxy-4-dibenzothiopheneyl)thio]-L-cysteinate. To a solution of 10.0 mg (0.0275 mmol) of 4-[(methoxycarbonyl)dithio]-6-acetoxydibenzothiophene in 0.5 mL of 5:1 dioxane–water was injected 4.9 μL (0.033 mmol, 1.2 equiv) of triethylphosphine. This solution was left under N_2 for 10 min, lyophilized, dried by azeotropic distillation with toluene (2×) and petroleum ether (2×), and placed under high vacuum for 1 h. The resulting pale yellow solid was dissolved in 0.7 mL of hexafluoroisopropyl alcohol, 0.1 mL of chloroform, and 0.1 mL of dioxane–water; to this was added under N_2 9.1 mg (0.028 mmol) of Boc-L-Cys(SScm)-OMe. After 20 min, the mixture was evaporated, dried by azeotropic distillation of CH_3CN then under high vacuum to afford a clear oil (19.2 mg), which was purified by preparative HPLC [eluent: 75:25 methanol–0.1% TFA (aqueous)], leaving a pale yellow solid after drying (10.4 mg, 0.020 mmol, 75%): TLC R_f = 0.56 in 9:1 $CHCl_3$–ethyl acetate; HPLC t_R = 5.70 min in 75% MeOH–25% 0.1% TFA (aqueous) (1 mL/min), t_R = 4.90 min in 95% MeOH–15% 0.1% TFA (aqueous) (1 mL/min); ^1H NMR (250 MHz, $CDCl_3$) 1.36 (s, 9 H), 2.39 (s, 3 H), 3.17 (m, 2 H), 3.66 (s, 3 H), 4.61 (d, 1 H), 5.26 (d, 1 H), 7.26 (d, 1 H, J = 8, C_3-H), 7.44 (t, 2 H, J = 8, C_2-H and C_8-H), 7.69 (d, 1 H, J = 8, C_7-H), 7.94 (d, 1 H, J = 8, C_1-H), 8.06 (d, 1 H, J = 8, C_9-H); mass spectrum (70 eV), m/e (relative intensity) 507 (M^+, 5), 464 (5), 351 (15), 232 (30), 391 (10), 451 (5), 57 (100).

D. Methyl *S*-[(6-Acetoxy-4-dibenzothiopheneyl)thio]-L-cysteinate (14). Failure To Establish an Intramolecular O,N-Acyl Transfer for 14. Following the procedure described for the preparation of the HCl salt of **13**, we subjected the Boc derivative prepared in step C to HCl in dioxane and then lyophilized it. The resulting hydrochloride was used immediately in acyl transfer experiments. Solutions of the hydrochloride salt of 14 in freshly distilled DMSO were prepared in the dark at concentrations in the range of (0.1–2.0) × 10^{-3} M and treated with 3–5 equiv of triethylamine in the presence of 5 mol % of $AgNO_3$ to suppress disulfide interchange. Comparison of HPLC analyses of the reaction mixture with those of independently synthesized product of the reaction showed no evidence for product formation during 20 h at 25 °C. During this time, unusually extensive disulfide interchange was noted which established a steady-state equilibration with symmetrical disulfides. After 265 h at 0.002 M initial substrate concentration, 3% conversion to product was detected. This can be attributed entirely to the intermolecular acyl transfer reaction. The reaction of 4-acetoxydibenzothiophene with H-L-Cys(Bzl)-OMe in DMSO at 25 °C was followed by HPLC under pseudo-first-order conditions over the amine concentration range of 0.2–1.4 M; second-order kinetics was observed with a rate constant of 9.7 × 10^{-5} M^{-1} s^{-1}.

Measurement and Estimation of Second-Order Rate Constants for Intermolecular Aminolyses. Although aminolysis reactions of phenyl esters in nonaqueous solvents frequently exhibit higher than first order dependences of rate on amine concentration, the solvent DMSO markedly accelerates ester aminolysis, presumably by assistance through hydrogen bonding of proton transfer from the amino group.[20,21] Not surprisingly, therefore, first-order dependence of rate on amine concentration is invariably seen in this solvent. This point has been proved by rate measurements under pseudo-first-order conditions over at least a 5-fold amine concentration range for the following cases: Z-Gly-ONp + H-Gly-OEt, 4-acetoxydibenzofuran + H-Cys(Bzl)-OEt, 4-acetoxydibenzothiophene + H-Cys(Bzl)-OEt, 1-acetoxyphenoxathiin + H-Cys(Bzl)-OEt, and 1-(Z-Ala-O)-phenoxathiin + H-Cys(Bzl)-OEt. It was assumed for all other cases. Rate measurements were usually carried out by HPLC, and frequently by NMR and UV spectrometry. Cysteine amines are unusually weak nucleophiles, even for peptide amines, and many of the phenolic esters that are appropriate models for the intermolecular reactions are exceptionally unreactive, even in DMSO. In order to avoid side reactions that arise with long reaction times, more reactive amines were used in several studies, and the amine reactivity differences observed in more tractable cases were used to estimate the rate constant for the cysteine case. The most reactive phenolic esters in this study were 4-acetoxydibenzothiophene and 1-acetoxyphenoxathiin. Under pseudo-first-order conditions over a concentration range of H-Cys(Bzl)-OEt of 0.05–0.3 M in DMSO at 25 °C, by HPLC monitoring of the disappearance of starting material and appearance of product, a strict second-order rate law was seen for 1-acetoxyphenoxathiin with a rate constant of 1.2 × 10^{-4} M^{-1} s^{-1}. Relative rates with this substrate under these conditions for H-Cys(Bzl)-OEt, H-Gly-OEt, and benzylamine were 1.0, 67, and 1.3 × 10^3, respectively. From two rate comparisons with H-Cys(Bzl)-OEt in the phenoxathiin and dibenzofuran series, the Z-Ala ester was 0.5–0.7 times as reactive as the acetyl ester. From a previous study with dibenzofuran derivatives,[3] a *p*-chloro substituent is known to accelerate the H-Cys(Bzl)-OEt aminolysis 12-fold.

The calculations of EM for **12** and **13** are reported elsewhere.[3] The appropriate intermolecular model for calculation of the EM for the intramolecular aminolysis of **11** is the reaction of 1,3-dimethoxy-2-methyl-5-acetoxyxanthone[10] with H-Cys(Bzl)-OEt at 25 °C in DMSO, which was followed by HPLC and UV methods to give an observed rate constant of 1.2 × 10^{-4} M^{-1} s^{-1}. Previously,[3] a 4-acetoxy-5-methyleneamidoxanthene was observed to react in

DMSO with H-Gly-OEt at 25 °C with a rate constant of 8.0×10^{-5} M^{-1} s^{-1}, which can be used to estimate a rate constant for the H-Cys(Bzl)-OEt reaction of 1.2×10^{-6} M^{-1} s^{-1}. Pseudo-first-order HPLC monitoring of the reaction of 4-(Z-Ala)-9,9-dimethylxanthene with H-Cys(Bzl)-OEt in DMSO at 25 °C gave a rate constant of 2.4×10^{-6} M^{-1} s^{-1} (D. Kemp and D. Buckler, unpublished observations). Accordingly, the appropriate second-order rate constant for modeling the EM of **10** lies in the range of $(1-3) \times 10^{-6}$ M^{-1} s^{-1}; values toward the high end of this range are more likely to be correct.

Like all small-ring cases, the modeling for the *o*-phenylene derivatives **8** and **9** is problematic, since the paired transition states almost certainly differ significantly. Possible models for **9** include the above-cited 4-acetoxydibenzothiophene (9.7×10^{-5} M^{-1} s^{-1}) and 1-(Z-Ala-O)-phenoxathiin (1.2×10^{-4} M^{-1} s^{-1}), which give an expected range for an *o*-thia-functionalized Z-Ala phenolic ester of $(6-12) \times 10^{-5}$ M^{-1} s^{-1}. Both models probably overestimate the rate constant owing to the electron-withdrawing meta functionality. An underestimate is provided by the more sterically constrained 1-acetoxy-2-(methylthio)naphthalene, which aminolyzes with benzylamine in DMSO at 25 °C with a rate constant of 1.6×10^{-3} M^{-1} s^{-1} (D. Kemp and F. Vellaccio, unpublished observations). Applying the appropriate corrections for the amine and the acyl function and a factor of 15–30 for the steric effect of the *peri*-8-naphthyl hydrogen, one estimates the model rate constant at 2.4×10^{-5} M^{-1} s^{-1}. Accordingly, the rate constant for modeling **9** probably lies in the range of $(2-5) \times 10^{-5}$ M^{-1} s^{-1}. A possible model for the intermolecular reactivity of an analogue of **8** is provided by 1-acetoxy-2-[(methylthio)methyl]benzene, which reacts with benzylamine in DMSO at 25 °C with a rate constant of 3.3×10^{-4} M^{-1} s^{-1} (D. Kemp and F. Vellaccio, unpublished observations). This can be translated into a rate constant of 2.1×10^{-6} M^{-1} s^{-1} for the reaction of the analogous Z-Ala ester with H-Cys(Bzl)-OEt. Almost certainly this rate constant is underestimated, so that a likely range is $(2-10) \times 10^{-6}$ M^{-1} s^{-1}. It should be noted that as a group the above rate constants fit one's expectation for the variations expected with small changes in the electron-donating and -withdrawing character of ortho and meta substituents.

X-ray Crystallography. X-ray data for **15** were collected at −65 °C on an Enraf-Nonius CAD4F-11 diffractometer using Mo Kα radiation. Data collection, reduction, and refinement procedures have been detailed elsewhere.[33] A total of 1440 reflections (h,k,l) were collected in the range $3° \leq 2\theta \leq 55°$ with the 1272 having $F_o > 4\sigma(F_o)$ being used in the structure refinement, which was by full-matrix least-squares techniques (181 variables) using HELX-76. Final $R_1 = 0.045$ and $R_2 = 0.052$. All hydrogen atoms, except the SH, were located in difference-Fourier maps; positional parameters and an isotropic temperature factor were refined for each H atom. Remaining atoms were refined anisotropically.

Crystal data are as follows: $a = 7.715$ (6) Å, $b = 8.643$ (3) Å, $c = 16.256$ (7) Å, $V = 1084.0$ Å^3, space group = $P2_12_12_1$, $Z = 4$, mol wt = 230, $\rho_{calcd} = 1.41$ g cm^{-3}, $\mu = 2.3$ cm^{-1}. An empirical absorption correction was applied.

Acknowledgment. We thank the Biomedical Research Support Shared Instrumentation Grant Program, Division of Research Resources, for funds to purchase the X-ray diffraction equipment (NIH Grant S10 RR02232). Financial support from Pfizer, Inc. and from the National Institutes of Health (GM R01 13453) is gratefully acknowledged. One of us (D.S.K.) acknowledges with gratitude the hospitalities of Prof. I. Ugi (T. U. Munchen) and Prof. J. Baldwin (Oxford University) and the financial support of the Alexander von Humboldt-Stiftung for a sabbatical year, during which many key elements of this work were pondered. Finally, we thank David Buchler for assistance with the energy calculations.

(32) Silverman, L. D.; Dewan, J. C.; Giandomenico, C. M.; Lippard, S. J. *Inorg. Chem.* **1980**, *19*, 3379.

(33) Press, W.; Flannery, B.; Teukolsky, S.; Vetterling, W. *Numerical Recipes—The Art of Scientific Computing*; Cambridge University Press: Cambridge, 1986; pp 52–63.

Appendix

Energy minimization was carried out with a program that has the following key features. Internal coordinates were used to describe atomic positions, and a "soft" energy minimization was carried out in which only torsional angles at the six single bonds of the backbone structure **20** are used as variables. Interatomic distances were calculated by using a recursive algorithm based on the law of cosines and the dihedral angle theorem. Externally fitted parity terms were used to determine the relative chiralities of summed dihedral angles. The six independent degrees of torsional freedom of **20** are reduced to two by the four independent constraints of fit to the template OS_2 and C_1C_2 distances and to the OC_1C_2 and SC_2C_1 angles. These two remaining degrees of freedom take the form of two independent, coupled torsional motions of the cysteine backbone under the constraint of attachment to a rigid template, and they can be expressed as linear combinations of rotations about all six torsional angles (inspection of a Dreiding model of structures such as **28** or **29** makes this point clear). For small motions for which a first-derivative Taylor expansion can accurately approximate the functions that express the distance and angle constraints as functions of the six backbone torsional motions, these two degrees of freedom can be calculated as follows. The six partial derivatives of OS_2, C_1C_2, and angles OC_1C_2 and SC_2C_1 with respect to the six torsional rotations of **20** are found for a particular template-bridging conformation of **20** by numerical differentiation. This set of 24 numbers defines a 4×6 matrix that has a two-dimensional null space spanned by the desired pair of orthogonal basis vectors. Application of a singular value decomposition algorithm[33] to this matrix provides the desired pair of 6-vectors.

One iterative loop of the computation follows the following sequence of operations. (1) Calculation of the distances and angles of template attachment for the given torsional angle values. (2) Calculation of distances from NH, α-CH, and β-CH atoms of the cysteine framework to four aryl carbons and the heteroatom of the template. Calculation of distances between the α-CH to ester O and cysteine S_2. (3) Calculation, using data of Allinger,[25,26] of van der Waals energies for each of the interactions found in step 2. Calculation of torsional strain, using the given torsional angles. (4) Calculation of the 4×6 matrix of first derivatives and, from it, the pair of null vectors. (5) Selection of a linear combination of null vectors that is added to the given torsional angles to form the set required for the second iteration.

The computations were run on an IBM PC AT microcomputer equipped with the mathematics coprocesser chip. One iterative sequence requires approximately 12 s of machine time, and a typical energy minimization required 80–100 iterations.

Registry No. **8**, 77834-01-6; **8**·HCl, 118143-66-1; **9**, 77834-03-8; **9**·HCl, 118143-67-2; **10**, 77834-02-7; **10**·HCl, 118143-68-3; **11**, 84310-90-7; **11**·HCl, 118143-69-4; **14**, 118143-43-4; **14**·HCl, 118143-70-7; **15**, 101697-55-6; Z-L-Ala-OH, 1142-20-7; Z-L-Ala-L-Cys-OMe, 34804-98-3; Z-L-Ala-L-Cys(2-HO-5-Cl-Blz)-OMe, 118143-45-6; Boc-L-Cys-OEt, 118143-52-5; Boc-L-Cys(SScm)-OMe, 118143-64-9; Z-Gly-ONp, 1738-86-9; H-Gly-OEt, 459-73-4; H-Cys(Bzl)-OEt, 953-18-4; 1-(Z-Ala-O)-phenoxathiin, 118143-72-9; 4-(Z-Ala)-9,9-dimethylxanthene, 118143-73-0; 2-hydroxy-5-chlorobenzyl alcohol, 5330-38-1; 5-chlorosalicylic acid, 321-14-2; 2-[[(methoxycarbonyl)dithio]methyl]-4-chlorophenol, 118143-42-3; 2-acetoxy-5-chlorobenzyl acetate, 6296-67-9; 2-hydroxy-5-chlorobenzyl mercaptan, 118143-41-2; (methoxycarbonyl)sulfenyl chloride, 26555-40-8; methyl *N*-(*tert*-butoxycarbonyl)-L-cysteinate, 55757-46-5; 2-mercaptophenol, 1121-24-0; cysteine disulfide, 118143-44-5; dimethyl LL-cysteinate, 1069-29-0; 2-hydroxy-5-

chlorobenzyl bromide, 117380-00-4; 4-hydroxy-5-(hydroxymethyl)xanthene, 118143-49-0; 4-hydroxy-5-formylxanthene, 75830-34-1; 4-hydroxy-5-[[(methoxycarbonyl)dithio]methyl]xanthene, 118143-50-3; 4-acetoxy-5-[[(methoxycarbonyl)dithio]methyl]xanthene, 118143-51-4; ethyl *N*-(*tert*-butoxycarbonyl)-*S*-[[(4-acetoxy-5-xanthenyl)methyl]thio]-L-cysteinate, 118143-53-6; bis(1,5-dihydroxy-3-methoxy-2-methyl-9-oxo-9*H*-xanthen-4-yl) sulfide, 118143-55-8; 1,5-dihydroxy-3-methoxy-2-methylxanthone, 118143-54-7; 2,3-dihydroxybenzoic acid, 303-38-8; 2-methyl-3,5-dimethoxyphenol, 50827-64-0; 1,5-dihydroxy-3-methoxy-4-[(methoxycarbonyl)dithio]-2-methylxanthone, 118143-56-9; ethyl *N*-(*tert*-butoxycarbonyl)-*S*-[(1,5-diacetoxy-3-methoxy-2-methyl-9-oxo-9*H*-xanthen-4-yl)thio]-L-cysteinate, 118170-28-8; 1,5-diacetoxy-3-methoxy-4-[(methoxycarbonyl)dithio]-2-methylxanthone, 118143-57-0; 1,5-diacetoxy-3-methoxy-4-mercapto-2-methylxanthone, 118143-58-1; 4-acetoxydibenzothiophene, 118143-59-2; dibenzothiophene, 132-65-0; 4-hydroxydibenzothiophene, 24444-75-5; 4-methoxydibenzothiophene, 24444-74-4; 4-methoxy-6-mercaptodibenzothiophene, 118143-60-5; 4-mercapto-6-hydroxydibenzothiophene, 118143-61-6; 4-[(methoxycarbonyl)dithio]-6-hydroxydibenzothiophene, 118143-62-7; 4-[(methoxycarbonyl)dithio]-6-acetoxydibenzothiophene, 118143-63-8; methyl *N*-(*tert*-butoxycarbonyl)-*S*-[(6-acetoxy-4-dibenzothiophene-yl)thio]-L-cysteinate, 118143-65-0; 4-acetoxydibenzofuran, 101762-27-0; 1-acetoxyphenoxathiin, 118143-71-8; 1,3-dimethoxy-2-methyl-5-acetoxyxanthone, 77834-07-2; 1-acetoxy-2-(methylthio)naphthalene, 118143-74-1; 1-acetoxy-2-[(methylthio)methyl]benzene, 54810-48-9; ethyl *N*-acetoxy-*S*-[[(4-hydroxy-5-xanthenyl)methyl]thio]-L-cysteinate, 118143-75-2; 2-[(methoxycarbonyl)dithio]phenol, 118143-46-7; methyl *S*-[(2-hydroxyphenyl)thio]-L-cysteinate, 118143-47-8; methyl *S*-[[2-[(benzyloxycarbonyl)-L-alanyloxy]phenyl]thio]-L-cysteinate, 118143-48-9.

Supplementary Material Available: Listings of final positional and thermal parameters and bonds and angles for **15** (20 pages). Ordering information is given on any current masthead page.

Reductive Ring Opening of *N*-Benzoylaziridine by Anthracene Hydride (Anion of 9,10-Dihydroanthracene) via Base-Induced Fragmentation of the Intermediate Carbonyl Adduct[1-3]

Helmut Stamm,* Thomas Mall, Reinhard Falkenstein, Jürgen Werry, and Dieter Speth

Pharmazeutisch-Chemisches Institut der Universität Heidelberg, Im Neuenheimer Feld 364, D-6900 Heidelberg, Federal Republic of Germany

Received August 8, 1988

As previously reported, reaction of anthracene hydride (AH^-), or of its oxa analogue xanthenyl anion (X^-), with *N*-benzoylaziridines **1a,b** can result in amidoethylation (**2a,b** and **3a,b**) of the carbanion, in reductive opening (**4a,b**) of the aziridine ring, and in attack on the carbonyl group of **1a,b**. We now show with **1a** that both the rate of ring opening and the amount of reductive opening are significantly enhanced by an excess of AH^-Li^+ while the initially formed (90%) carbonyl adduct **6a** survives with a deficit of AH^-Li^+. Both effects due to carbanion excess are absent with X^-Li^+ but are much stronger with AH^-Na^+. These results point to a rapid process that is triggered off by deprotonation at position 10 of the carbonyl adduct **6**. A concerted or subsequent homolytic fragmentation is proposed to generate the ketyl **5** of **1**, followed by homolytic ring opening of **5** to yield the radical **12**, which is reduced to the carbanion **14**. The latter forms **4** by capturing a proton from dihydroanthracene. Inaccessibility of reductive ring opening for a trialkylacetyl-activated aziridine is demonstrated again (**18**).

Ring opening of *N*-aroylaziridines, e.g., **1a,b** by anthracene hydride (AH^-) (or xanthenyl anion (X^-)) can provide[4] amidoethylated dihydroanthracenes such as **2a,b** (or amidoethylated xanthenes, e.g., **3a,b**) and products of reductive opening, e.g., **4a,b** (Chart I). Both types of products were proposed to arise by homolytic ring opening of an intermediate ketyl, **e.g., 5a,b**.[4] Ring opening was preceded by the formation of a carbonyl adduct such as **6a,b** (or **7a,b**) as evidenced by the isolation of ketones of type **8** or **9** in high yield when the reaction could not go to completion.[4] A strong influence of the gegenion (Li^+ or Na^+) of X^- was described in a recent paper[3] together with a trapping of AH^-, X^-, and **1a** under reaction conditions that normally give the ketones **8** or **9**. Consequently, the carbonyl adducts **6a** and **7a** are reversibly formed by a classic ionic mechanism and the equilibrium concentrations of **1a** and X^- (and by analogy of **1a** and AH^-) are responsible for the ring-opening reactions: amidoethylation (forming **3a** and by analogy **2a**) and, to a negligible extent (ratio **3a:4a** = 8:1),[3] reductive opening. The latter is a slow process and proceeds most likely by single-electron transfer (SET) from X^- to **1a** forming **5a** and the radical $X^\bullet$ (analogously AH^- may form **5a** and the radial $AH^\bullet$). The respective conclusions can be applied to other *N*-benzoylaziridines. Since the dimethylaziridine **1b** undergoes only abnormal opening (**2b, 3b, 4b**),[4] this points to an SET mechanism[5] at least in this case where steric hindrance slows down the S_N2 ring opening.[5] On the other hand, the S_N2 path to **2a** and **3a** cannot be ruled out. Now, there are two findings that point to a different behavior of AH^- and X^-, which is not accounted for by the previous[4,3] interpretations. In the first reported[4] ring-fission reactions of **1a,b**, reductive opening was the main event with AH^-, but it was a side reaction with X^-. Second, the reported ring opening of **1a** proceeded much faster[3] with AH^-Li^+ than with X^-Li^+. We now present evidence that base-induced fragmentation of the carbonyl adduct

(1) Reactions with Aziridines. 49. Arene Hydrides. 6.
(2) Reactions with Aziridines. 48; see: Stamm, H.; Onistschenko, A.; Buchholz, B.; Mall, T. *J. Org. Chem.* **1989**, *54*, 193–199. 47: Stamm, H.; Speth, D. *Arch. Pharm. (Weinheim)*, in press. 46: Mall, T.; Stamm, H. *Chem. Ber.* **1988**, *121*, 1353–1355.
(3) Arene Hydrides. 5. Reactions with Aziridines. 45: Mall, T.; Stamm, H. *Chem. Ber.* **1988**, *121*, 1349–1352.
(4) Stamm, H.; Sommer, A.; Woderer, A.; Wiesert, W.; Mall, T. *J. Org. Chem.* **1985**, *50*, 4946–4955.
(5) Stamm, H.; Assithianakis, P.; Buchholz, B.; Weiss, R. *Tetrahedron Lett.* **1982**, 5021–5024.

0022-3263/89/1954-1603$01.50/0